Design of a Double Cantilever Based Interferometric Bio-Sensor

By
Dean Berlin, Jain Li, Cagri Savran, Joachim Sihler, Wan-Chen Wu
Prof. Martin Schmidt, Prof. Scott Manalis

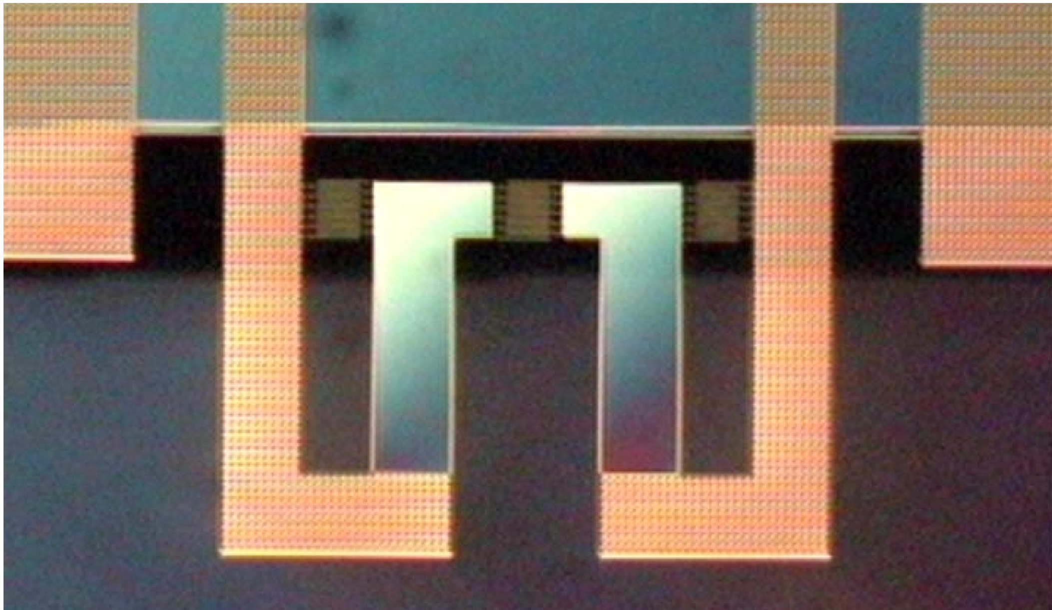

6.151 Semiconductor Devices Laboratory
Massachusetts Institute of Technology

Spring 2001

CONTENTS

1 INTRODUCTION **3**

2 BACKGROUND **3**
2.1 Bending of cantilevers caused by different mechanisms of molecular adsorption ……………… 3
2.2 Advances in metrology for detecting the tip deflection of micro cantilever bending …………… 11

3 HIGH LEVEL DESIGN **13**
3.1 Overview ………………… ……………………………………………………………….. 13
3.2 Interdigital fingers for deflection movement ……………………………………………… 13
3.3 Double cantilevers for signal noise reduction ……………………………………………… 14
3.4 Device Sketch ……………………………………………………………………………….. 15
3.5 Fluidic System ……………………………………………………………………………… 16

4 DOUBLE CANTILEVER **18**
4.1 Detailed design ……………………………………………………………………………... 18
4.1.1 Cantilever design …………………………………………………………………… 18
4.1.2 Interdigital finger design …………………………………………………………… 20
4.1.3 Combination of the cantilevers and the Interdigital sensor …………………………… 21
4.2 Fabrication and results ……………………………………………………………………… 22
4.3 Recommendations and conclusions ………………………………………………………… 35

5 MICROCHANNEL DESIGN AND FABRICATION **37**
5.1 Design ……………………………………………………………………………………….. 37
5.2 Fabrication and results ……………………………………………………………..……….. 40
5.3 Recommendations and conclusions ………………………………………………………… 47

APPENDIX **52**
PDMS Microchannel Fabrication Process Flow

REFERENCES **59**

1 INTRODUCTION

In February 2001, a MEMS design problem was presented to us related to the field of BioMEMS. The task was to design a cantilever based sensor device than can be used for various biochemical analysis applications. In recent years, biosensors have been developed that take advantage of the bending effect of micro-cantilevers due to molecular adsorption on the surface. The deflections of the cantilever tips are typically on the order of 10-100nm. The displacements have been measured with laser beam deflection techniques using position sensitive diodes which require sensitive alignment. Fundamentally new metrology methods for this application use diffraction grating techniques which are significantly simpler and less sensitive to misalignment.

The device we built combines the advantages of diffraction grating interferometry and differential data acquisition for noise reduction into a compact double cantilever design. The cantilevers and support structures are U-shaped to simplify dipping the device into liquids. For this special purpose, we made a custom pipette device fabricated in a side project. The pipette device consists of two fluid reservoirs that terminate in adjacent fluid spouts which allows submersion of the two halves of the cantilever device in two different fluids.

2 BACKGROUND

2.1 Bending of cantilevers caused by different mechanisms of molecular adsorption

Within the last few years, advances in biomedical and chemical sensor technology based on micro-cantilevers have been reported. It has been observed that certain adsorbtion effects of molecules on the cantilever surface can cause either tensile or compressive surface stress and therefore bending of the cantilever. Typically, one side of the cantilevers is coated with gold due to its high affinity to molecular bonding. A number of the reported experiments (see table 2.1) use commercially available cantilevers such as those used for AFM tips. These cantilevers are mostly V-shaped (for more stiffness against lateral bending) and their dimensions are typically 200 microns in lenth, 40 microns wide (each of the V-shaped legs), and about 0.6 microns thick. Other experiments use custom fabricated straight cantilevers with similar dimension. The small size of these cantilevers is ideally suited for these applications for several reasons. First, the sensitivity of the cantilever increases linearly with the length to thickness ratio. Using microfabrication techniques, cantilevers can be made of extremely thin films with a thickness on the order of 1 micron or less. Second, small cantilevers can give reasonably fast respones without reaching the domain of the first few natural frequencies. Finally, the amount of analyte needed for detection decreases with the reactive cantilever surface area and traces of analytes can be detected beyond the resolution of “classical” methods [7].

Table 2.1: This table provides a comparative view of a selection of papers from research groups that have reported advances in sensor technology based on cantilever bending.

Article	Baller et. al. ”A cantilever based artificial nose”	Moulin et. al. “Measuring Surface-Induced Conformational Changes in Proteins”	Raiteri et. all. ”Changes in Surface Stress…measured with a micro cantilever	Fritz et. al. “Translating Biomolecular Recognition into Nanomechanics”	Fritz et. al. “Stress at the solid-liquid interface of Self-assembled monolayers…”	Hai-Feng et. al. “Detection of PH variation using modified microcantilever sensors”	Wu et. al. “Chemical Sensing in Fourier Space	Thaysen et. al. “cantilever based bio-chemical sensing…”
date	08/17/1999	09/20/1999	11/04/1999	04/14/2000	10/13/2000	10/16/2000	12/11/2000	Jan-01
Cantilever	Si 30nm gold 5nm polymer	Si3N4 V-shaped (AFM tip) gold layer	Si3N4 V-shaped (AFM tip) 3-5nm Cr 30-40 nm gold	Si gold layer	Si 1nm Ti 20nm Gold	Sio2, Si3N4 3-8 Cr 20nm gold	SiNx	Si/SiN 40nm gold
Length [um]	500	200	190	500	500	200	300	125
Width [um]	100	36 (legs)	40 (legs)	100	100	40 (legs)	12	40
Thickness [um]	1	0.6	0.6	1	1	0.7	1	0.52
Max. deflection	N/A	N/A	N/A	100 nm	100 nm	500 nm	N/A	N/A
Surface stress [N/m]	<0.1	N/A	-0.05…0.15	0.005	0.032	N/A	N/A	5 N/m
Bending mechanism/ experiment	Swelling of polymers upon exposer to gaseous analytes	Protein adsorption on gold surface	pH-detection	DNA-hybridization, receptor-ligand binding	pH-detection	pH-detection	Chemical vapor sensing, remote temperature detection	Immobilization of single-stranded thiol modified DNA-oligos, Aqua regia etch of gold
Measuring method	Optical beam deflection technique	Optical beam deflection technique	Optical beam deflection technique	Optical beam deflection technique	Optical beam deflection technique	Optical beam deflection technique	Optical diffraction	Piezo resistive; resolution 2.6mN/m

In order to monitor the surface stress changes during the self-assembly of an alkanethiol monolayer, Berger et.al. [8] evaporated a few microliters of alkanethiol onto the gold surface of an AFM cantilever tip and measured the tip deflection by capturing a reflected laser beam with a position sensitive diode (fig 2.1.1).

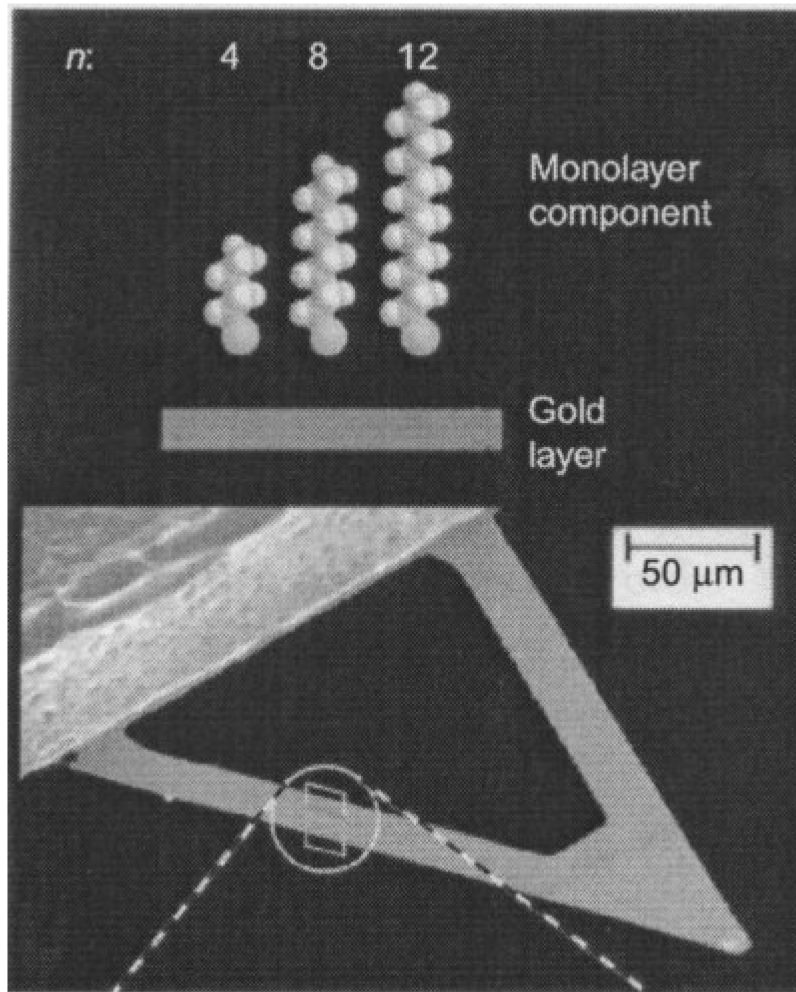

Fig 2.1.1

Other possible applications for cantilever based sensors include "artificial noses", as shown in [7]. An array of cantilevers (fig 2.1.2) has been functionalized with different types of polymers (fig 2.1.3).

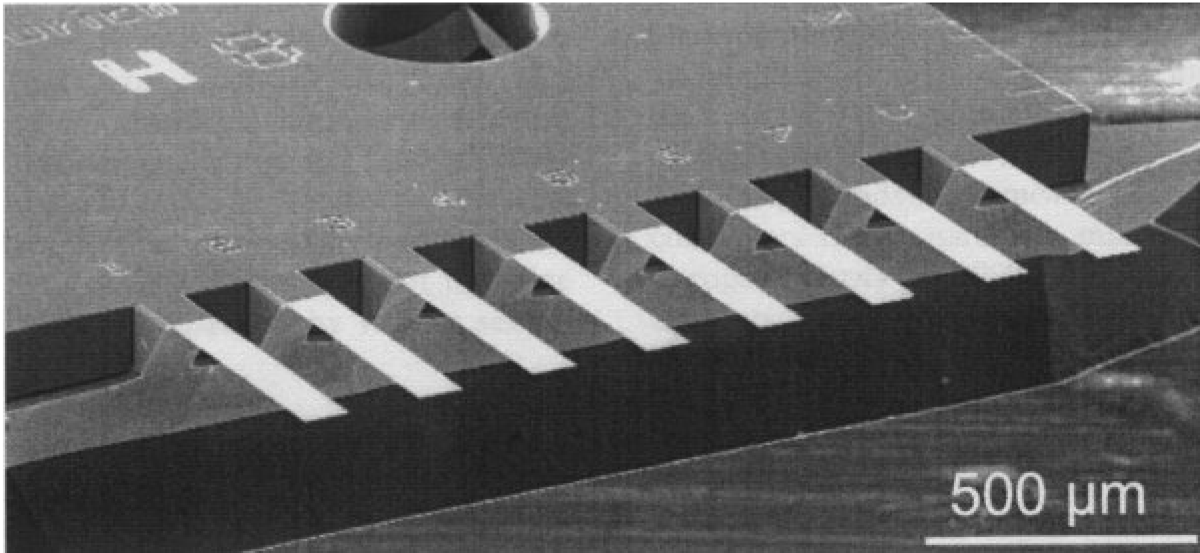

Fig 2.1.2

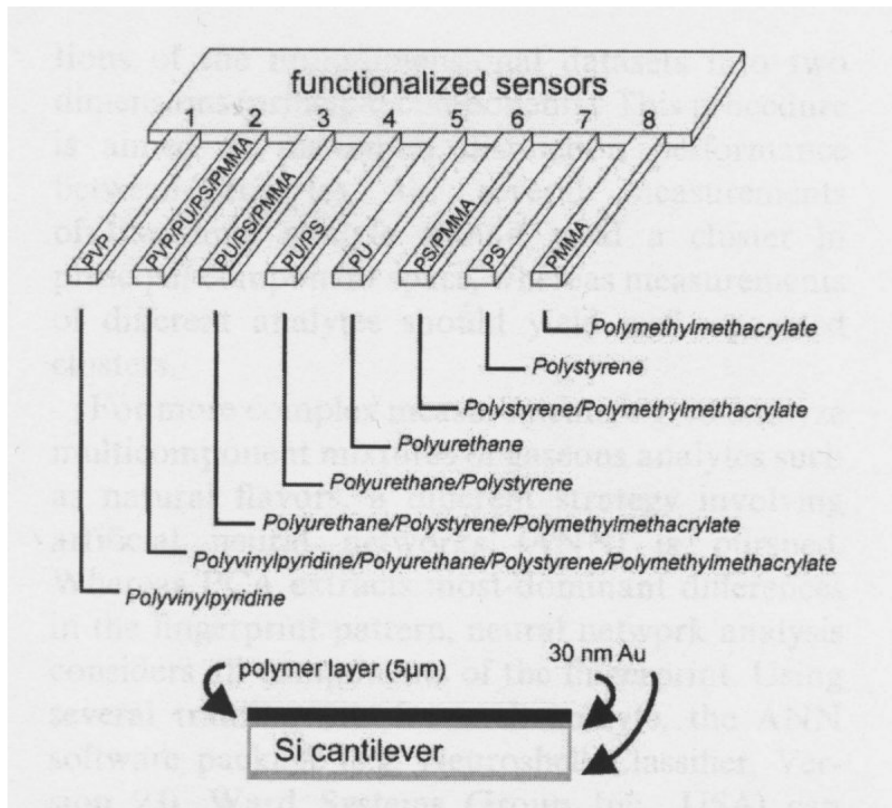

Fig 2.1.3

Exposure to gaseous analytes will cause a swelling effect of the polymers which cause bending. The bending was picked up with an optical beam deflection technique: a laser beam which bounces off the tip of the cantilever hits a position sensitive diode. The cantilevers are made of silicon and they are coated with a 30nm layer of gold prior to functionalizing with polymers.

Moulin et. al. [9] used a gold coated micro cantilever (fig 2.1.4) to examine the kinetics of protein adsorption on solid surfaces, which is of importance for understanding for example the interaction of living tissue with artificial implant, such as heart valves, kidney implants, or contact lenses.

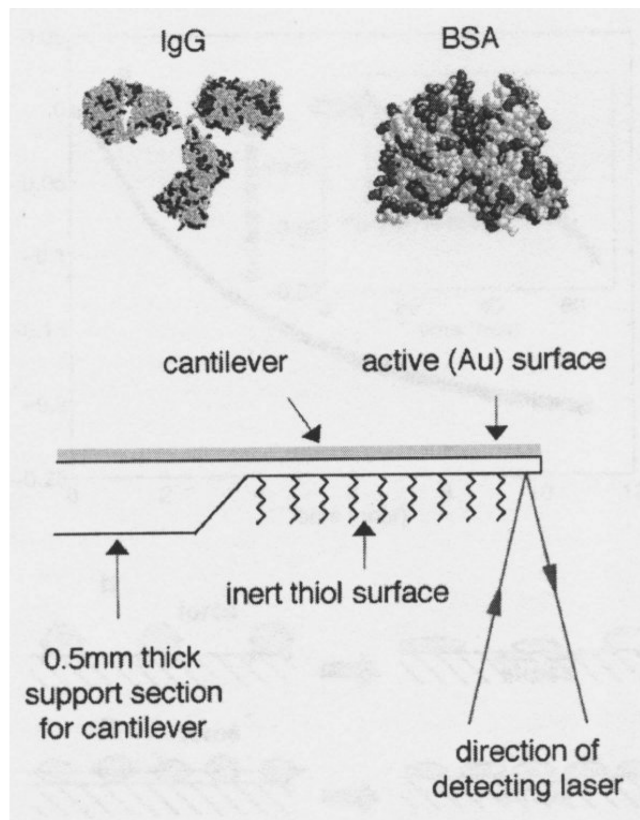

Fig 2.1.4

A commercially available AFM tip cantilever was coated with a gold layer on one side to promote the adsorption of immoglobulin (IgG) and albumin (BSA). The backside of the cantilever was coated with the thiol $HS(CH_2)_{10}(CO_2C)_2COCH_3$ in order to reject any kind of proteins. This will guarantee the adsorption of proteins only on one side of the cantilever and hence maximize the surface stress and the deflection of the cantilever. Adsorption of IgG was found to be compressive whereas adsorption of BSA was found to be tensile.

In another experiment reported by Raiteri et. al. [10] the bending of cantilevers was used to create a pH value sensitive device. The cantilever surfaces were coated (fig 2.1.5) with monolayers of octadecanethiols and 3-mercaptoprionic acid, respectively.

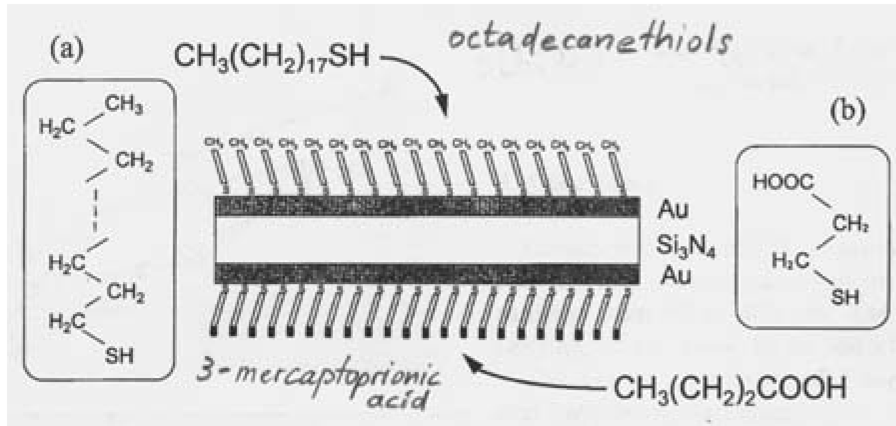

Fig 2.1.5

The tip deflection was picked up by laser beam deflection technique (fig 2.1.6). The bending mechanism was explained by the fact that the carboxyl group in the 3-mercaptoprionic acid can loose a proton (H+) and therefore charge themselves which increases the surface energy.

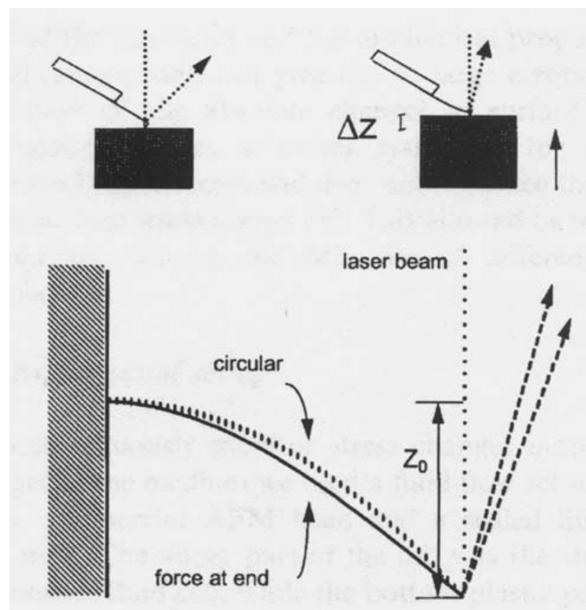

Fig 2.1.6

An interesting application of a cantilever based biosensor was examined by Fritz et. al. [11]. DNA hybridization and receptor-ligand binding was directly transduced into a bending response of an array of mircofabricated cantilevers (fig 2.1.7).

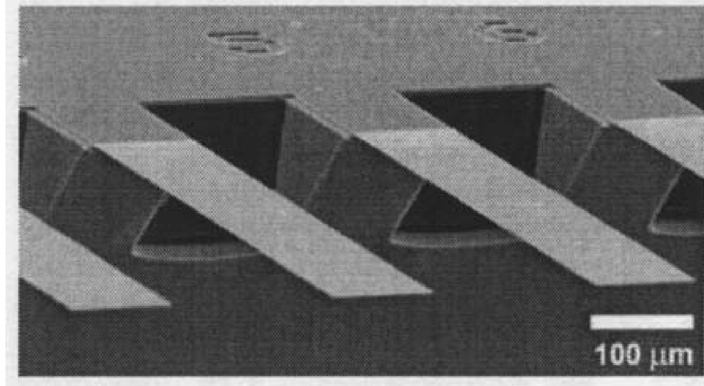

Fig 2.1.7

The cantilevers were made of silicon with a layer of gold on one side. In a first hybridization experiment (fig 2.1.8), a monolayer of 12-mer oligonucleotides was immobilized on one cantilever, whereas a monolayer of 16-mer oligonucleotides was immobilized on the other cantilever.

Fig 2.1.8

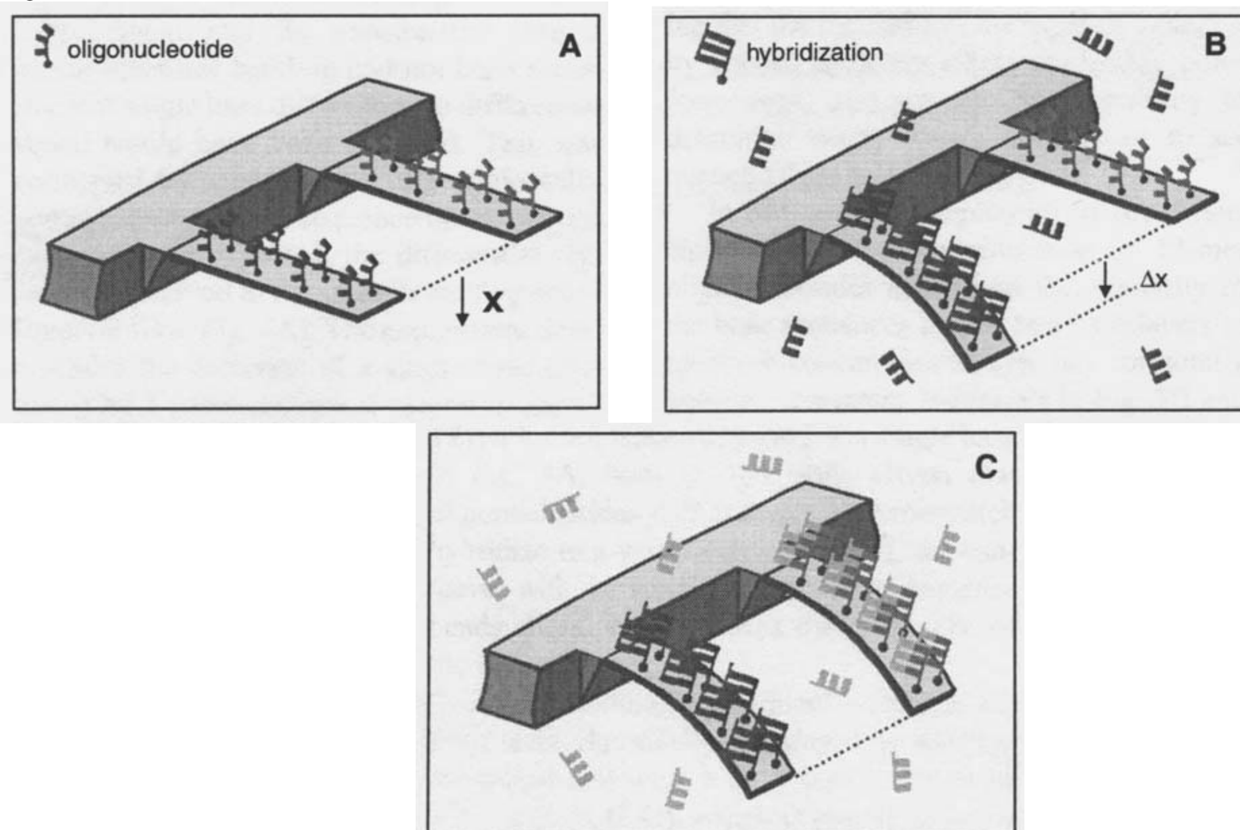

Injection of the complementary 12-mer and 16-mer oligonucleotide solutions led to a hybridization reaction of the oligonucleotides in solution and the resulting difference in surface stress between the gold coated layer and the uncoated Si backside caused bending of the cantilever. In order to eliminate noise from the data, Fritz et. al used a differential method (fig 2.1.9)by subtracting the bending signal of the two mechanically identical cantilevers.

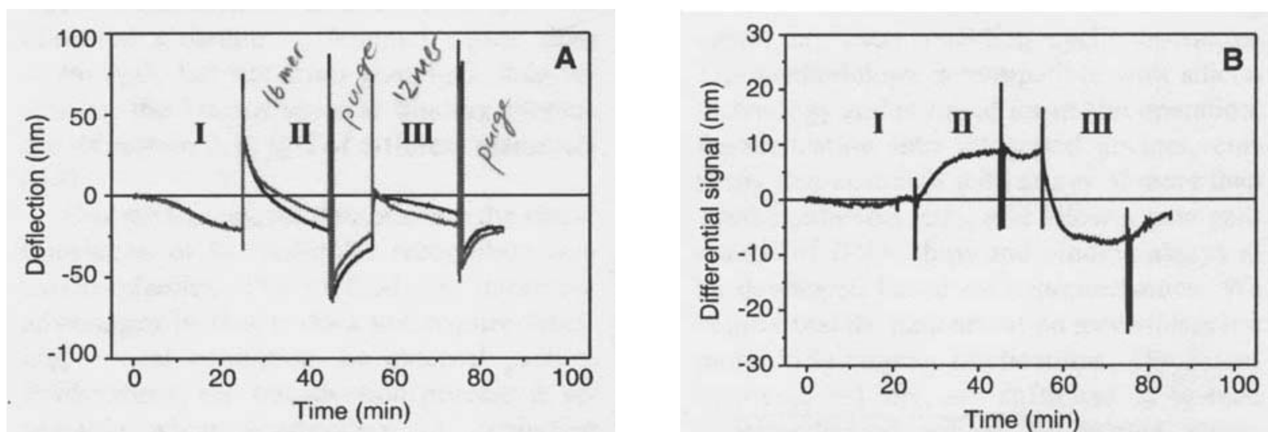

Fig 2.1.9

In another experiment it was demonstrated, that 12-mer oligonucleotide with a single base mismatch can be detected with this method. In order to further demonstrate the applicability of this method, the binding of immunoglobulins (IgG) to protein A was done on a cantilever surface, which also caused measurable bending deflections.

In another paper by Fritz et. al. [12], the pH value measurement of a buffer solution was demonstrated. The cantilevers were thiol modified and the bending signal dependent on the pH value was acquired using a differential method to compensate for changes in temperature and refractive index of the liquid environment.

Ji et. [13] al. also experimented with micro cantilevers to detect the pH value. They used SiO2 and Si3N4 cantilevers with chemically modified surfaces and picked up the tip deflection using a reflected laser beam and a position sensitive photo diode.

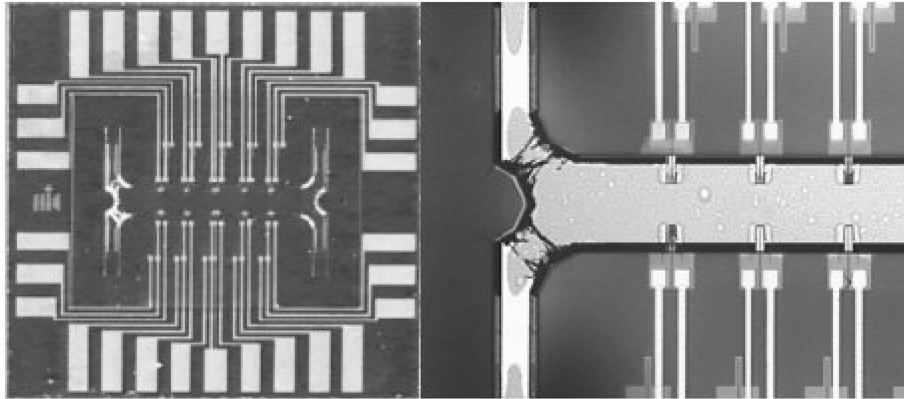

Fig 2.1.10

Thaysen et. al. [3] designed a micro cantilever array (fig 2.1.10) with a new piezo resistive detection system (fig 2.1.11)that was used to monitor the changes in surface stress during the aqua regia etch of the gold layer.

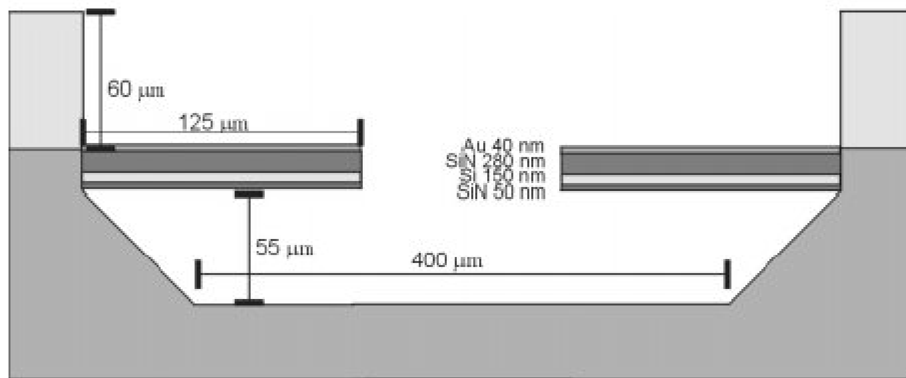

Fig 2.1.11

In another experiment, the same cantilevers were used to pick up the bending deflection due to the immobilization of thiol modified DNA-oligos (fig 2.1.12). The piezo resistive measuring system has advantages regarding the simplicity and the possibility to directly obtain electric signals from non-transparent liquids.

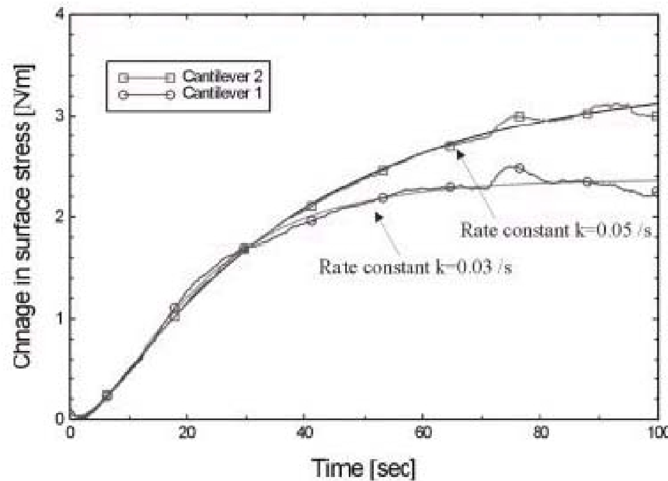

Fig 2.1.12 *Surface stress changes as a function of time when a sample of thiol modified DNA-oligos are flowing in the channel. The DNA-oligo solution is introduced in the channel at t=0 seconds. The graphs both follow an Langmuir type adsorption model (smooth curves).*

2.2 Advances in metrology for detecting the tip deflection of micro cantilever bending

[14], [15], [16], [17], [4] report the application of a new detection method for micro cantilever bending. The technique uses a set of secondary reflective fingers arranged in an interdigital pattern (fig 2.2.1).

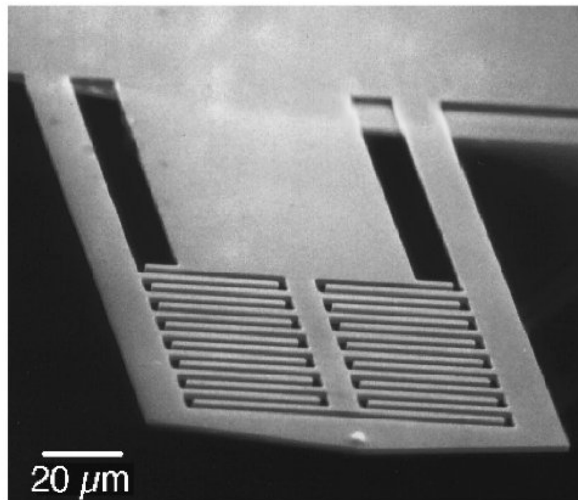

Fig 2.2.1

The fingers are typically attached to the cantilever tip and when the cantilever bends, every second finger will move vertically out of plane (fig 2.2.2).

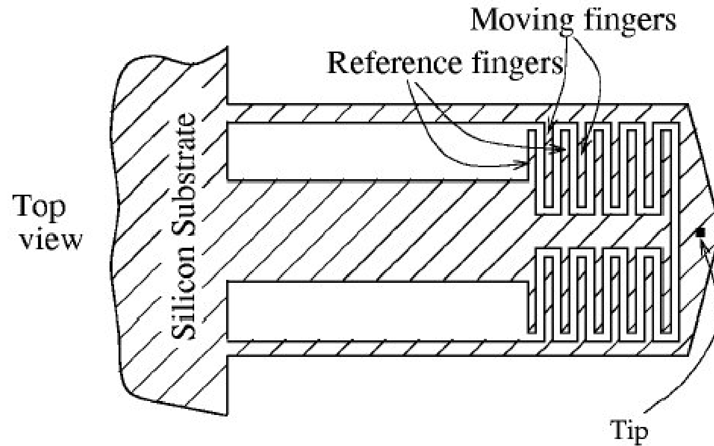

Fig 2.2..2

The reflection of a beam of coherent light will show changes in the diffractive pattern (figure 2.2.3). The light intensity of the 0th mode of diffraction will decrease as the fingers move out of plane. A finger travel of 1/4 of the wavelength of the laser light will result in a full destructive interference completely canceling the 0th mode. The major advantage of this method compared with the widely used optical beam deflection technique is that only the light intensity, not the position of the reflected laser beam needs to be measured. This eliminates many alignment issues and it also allows to easily transduce the bending signal by means of a simple photo diode.

Fig 2.2.3

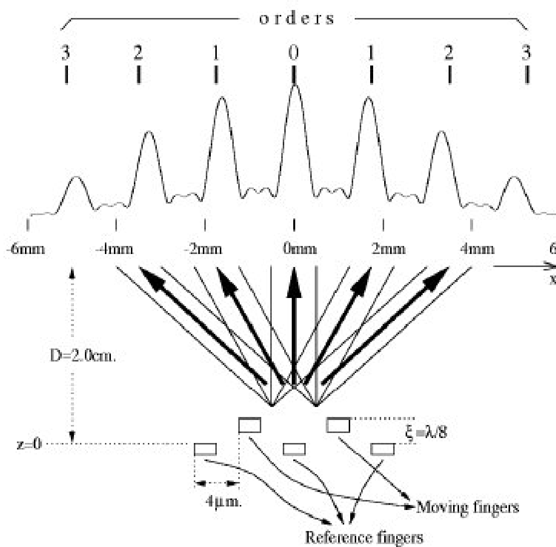

FIG. 4. Cross-sectional view of the grating. The width of the fingers are 2 μm. Spatial frequency of the grating is $f_g = 5\times 10^5$ m^{-1}.

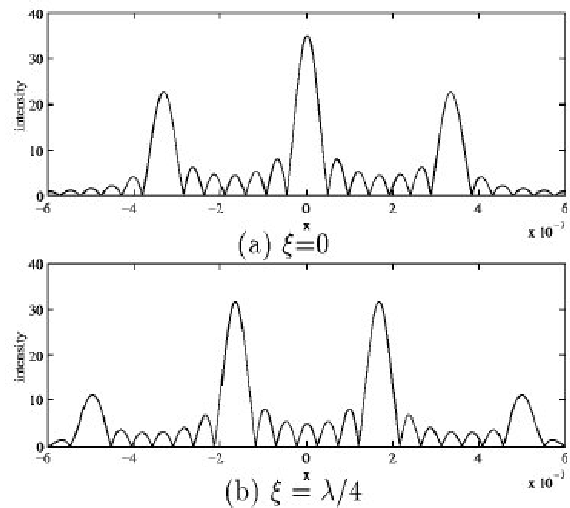

FIG. 5. Field intensity at $D=2$ cm. Fingers are assumed to be infinitely long.

3 HIGH LEVEL DESIGN

3.1 Overview

Recently, a number of new biochemical sensors technologies have been developed based on cantilever bending. The bending is caused by a change in surface stress due to the adsorption of molecules on one side of the cantilever, such as DNA hybridization or protein adsorption. Some of the reported experiments use an optical beam deflection method ("optical lever") to detect the cantilever tip displacement. This requires a very well aligned position sensitive photo diode. A more simple technique uses a set of interdigital fingers attached to the cantilever tip to generate a diffraction pattern. Bending of the cantilever changes the diffraction light intensity which can be detected with a photodiode. In order to eliminate noise from the signal, differential methods have been successfully applied using two mechanically identical cantilevers.

The goal of this project is to design and fabricate a double cantilever sensor device useful for biomolecular analyses, which combines the two methods mentioned above. The two cantilevers are equipped with a total of 3 sets of interdigital gratings that allow absolute as well as differential readout of the cantilever tip displacements.

3.2 Interdigital Fingers for Deflection Measurement

The reflection of a laser beam focused on the interdigital gratings (Figure 3.2.1) will form a diffraction pattern.

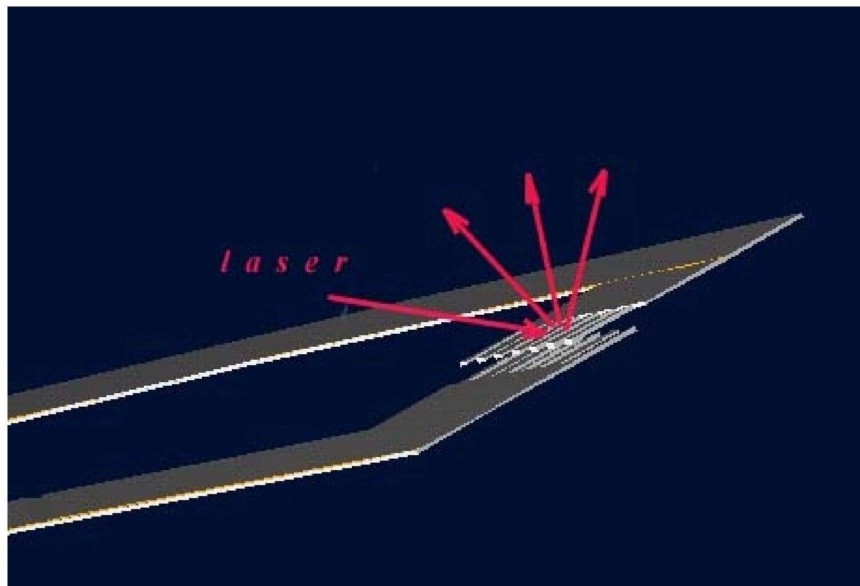

Fig. 3.2.1.: Differential Deflection of the two Cantilevers and Diffraction

The light intensity distribution of this pattern depends on the relative position of the moving versus the reference fingers (Figure 3.2.2). If all fingers are in plane (undeflected cantilever), the 0th mode will have maximum intensity. Out of plane movement of the moving fingers will cause the intensity of 0th mode to decrease. A finger travel of 1/4 wavelength of the laser light will completely cancel this mode. Consequently, a simple photodiode which detects the light intensity of the 0th mode can be used to directly infer the cantilever displacement.

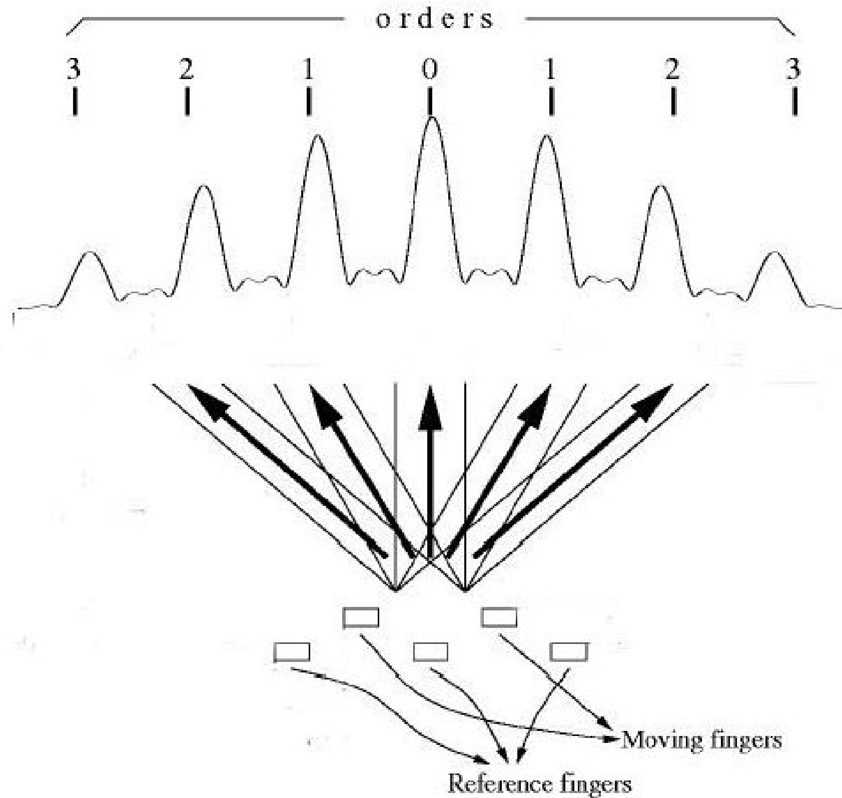

Fig. 3.2.2.: Diffraction Pattern Intensity Distribution

3.3 Double-Cantilevers for signal noise reduction

Environmental factors such as heat, vibration, turbulence, etc. can cause significant noise and drift in the deflection signals of individual cantilevers. Signals from DNA hybridization, for example, can be sufficiently small so that their detection becomes quite difficult. This problem can be solved by exposing two cantilevers of the same kind to the same conditions and recording the differential displacement bending deflection signal. In Fritz's experiments, individual cantilever signals showed a deflection drift of several tens of nanometers and spikes of up to 100 nm while the useful signal was only about 10nm. Through differentiating the signals of two cantilevers, the drift was reduced to 1~2nm.

3.4 Device Sketch

In order to extract differential as well as absolute displacement signals, our double cantilever device is equipped with a total of 3 sets of interdigital fingers (Figure 3.4.1.). The reference fingers of the outside sets are attached to the honeycomb supported base and are therefore fixed with respect to ground. This will allow to measure the absolute displacement of each cantilever. The diffraction grating measurement of the finger array between the two cantilevers will provide a signal corresponding to the difference in bending. This represents a direct mechanical way to generate the differential signal.

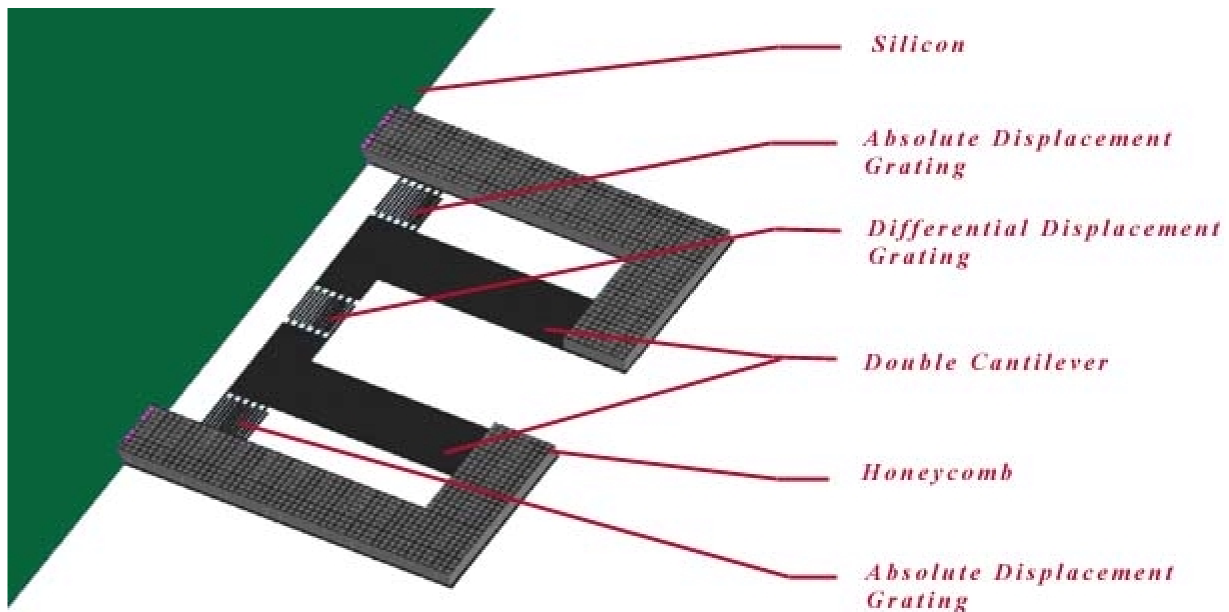

Fig. 3.4.1.: Backside view of the Double-Cantilever

The crossing rib reinforcement structure is formed by initially etching crossing trenches into the silicon substrate. Then, we deposit a 1 micron thick silicon nitride layer, which should fill the 2 micron wide trenches and thereby leave a top layer with ribs underneath. The "honeycomb" rib structure will be exposed after selectively removing the silicon through an anisotropic etch in KOH. The U shaped cantilever are formed by plasma etching, which is done before the KOH release.

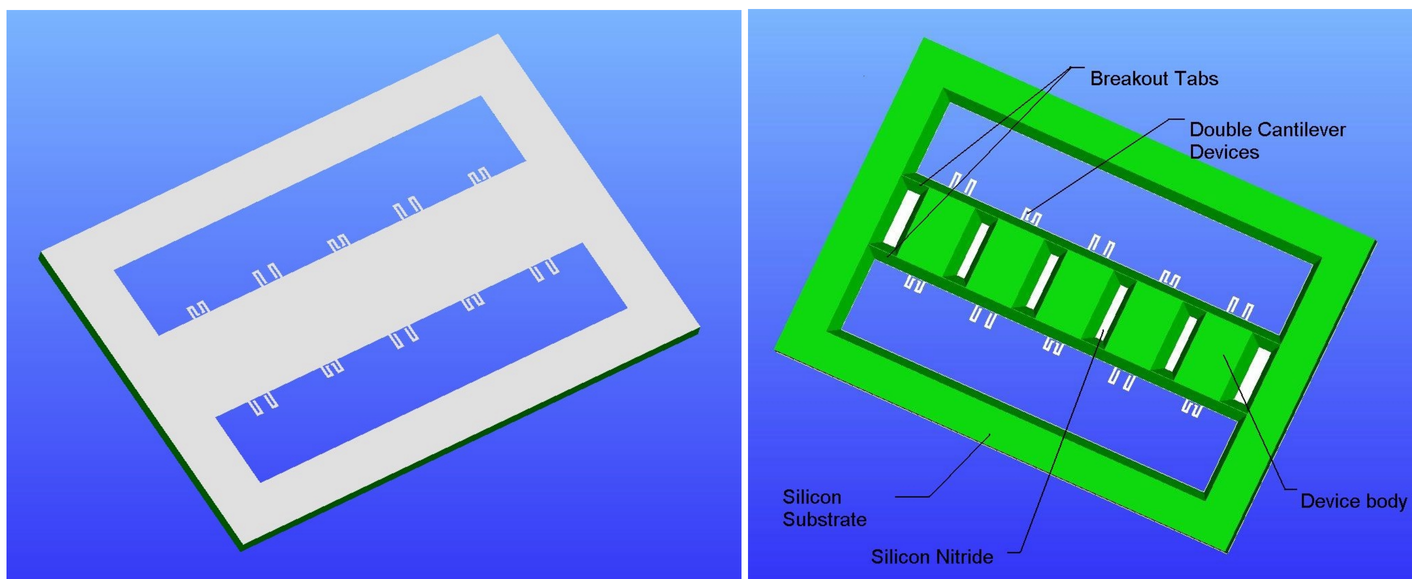

Fig. 3.4.2.: Front and backside view of a wafer die

Figure 3.4.2. shows how we arranged the devices in a die. Each die consists of 5 device bodies that have one double cantilever device attached to each end. For analytical purposes, the devices themselves have different sizes and diffraction grating arrangements. The figures actually show the devices after the KOH release; the slanted sidewalls are due the anisotropic etch. The front- and backside masks were designed such that after KOH etch, the individual device bodies would only be connected by small tabs. The devices can be easily released from the substrate by breaking the tabs. A detailed description of the fabrication can be found in Section 4.2.

3.5 Fluidic System

For biochemical analyses, the double cantilever device will have to be submerged into different kinds of fluids. For DNA hybridization for example, each one of a pair of cantilevers has to be dipped into different oligonucleotide solution. Since we didn't want to be constrained in our design by the size of commercially available pipette tips, we decided to custom make a fluidic device that can be used with the cantilevers. This fluidic system consists of a pair of reservoirs that can be filled with the desired liquids. Small flow channels lead the liquid to a special tip which is compatible in dimensions with the double cantilever device. The two liquids are being kept separate all the way up to the tip. The fluidic device is made of PDMS, a special polymer that can be mixed and pored onto a mold in liquid form. The mold is made using a carrier wafer and a layer of SU-8 which was structured using standard photolithography. Figure 3.5.1. shows how the double cantilever and the fluidic system are supposed to work together.

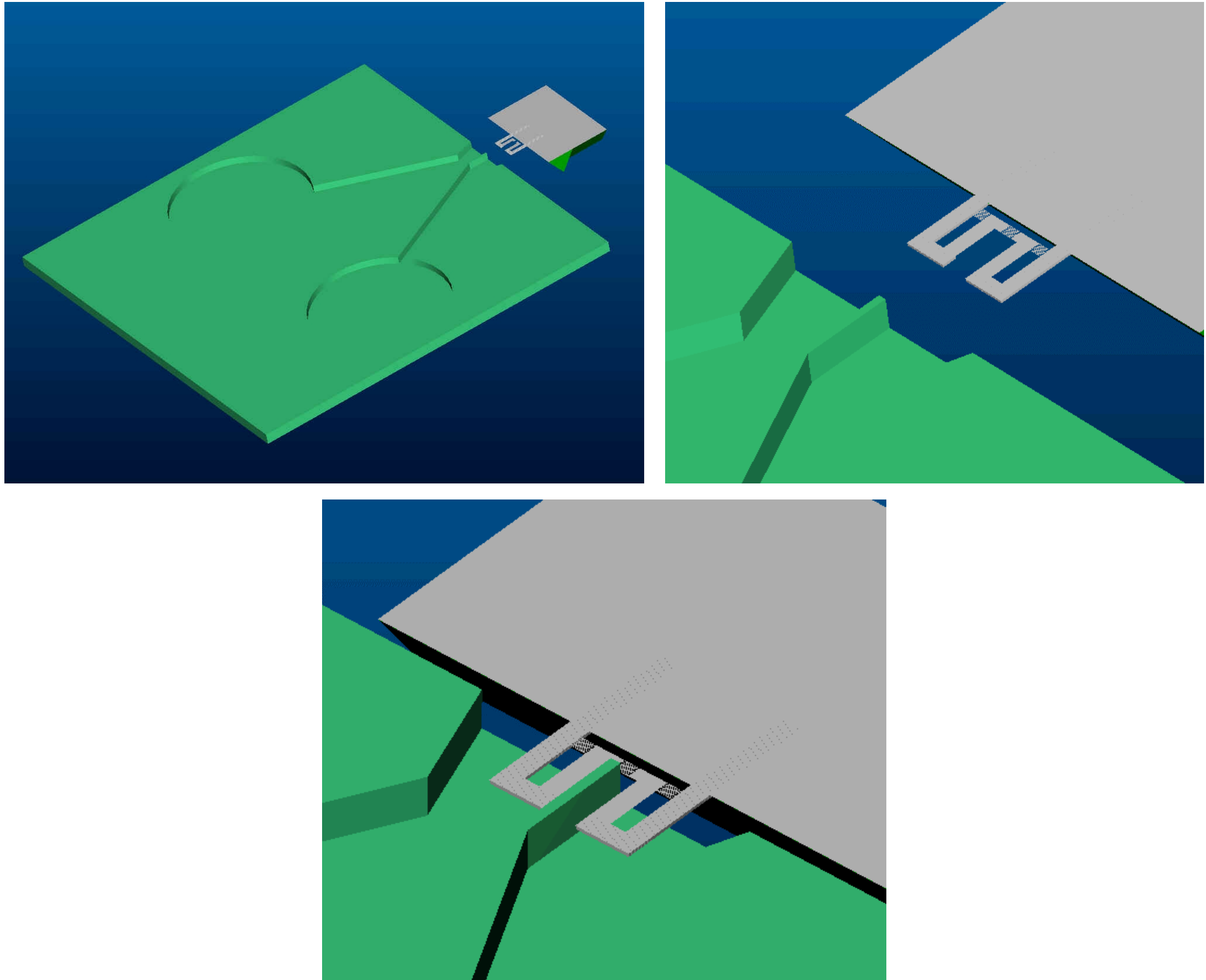

Fig. 3.5.1.: Dipping the Device into Fluid

4 DOUBLE CANTILEVER

4.1 Detailed Design

In this section, we discuss the detailed design of the double cantilever system and the accompanying interdigital displacement sensor

4.1.1 Cantilever Design

As discussed earlier, the goal of the study is to design a more robust and sensitive version of the dual cantilever system that had been successfully fabricated and tested by Fritz et. al. [2] Hence, we used their work as a foundation for our design.

Fritz et. al. built a pair of silicon micromachined cantilever beams to study hybridization of DNA strands. The dimensions of beams were $L = 500\mu m$, $w = 100\mu m$, and $t = 1\mu m$, where L, w, and t represent the beam length, width and thickness respectively. Top sides of the beams were covered with gold. One beam was functionalized with single-strand 16-mer, and the other with 12-mer oligonucleotides. Functionalization was achieved by the covalent immobilization of the thio-modified oligonucleotides on the gold-covered surface. The complementary 16-mer and 12-mer oligonucleotides were then injected sequentially, to hybridize the oligonucleotides that had previously self-assembled on the cantilever surfaces. The beams deflected on the order of $10nm$ due to the surface stress caused by the hybridization. The relation between the surface stress and the beam's tip deflection is given by the well-known Stoney's equation:

$$\sigma = \frac{Et^2}{4L^2(1-\nu)}\Delta z \tag{4.1}$$

where E,ν, and Δz are Young's modulus, Poisson's ratio and the beam's tip deflection respectively. The deflection, caused by this hybridization-induced surface stress was measured on both cantilevers by means of two laser beams focused on the tips of the beams. Since the two cantilevers accommodated oligonucleotides of different lengths, their tip deflections were slightly different. Taking the difference of the signals from the two cantilevers minimized the effect of thermal noise on the measurement, since such an effect would be almost the same on both cantilevers.

In light of this study, our design was also focused on building a pair of identical cantilevers and measuring the difference in the signals generated by the deflection of the two cantilevers. However, instead of measuring the deflections of the beams individually and subtracting the signals, as in the study of Fritz et. al., our design incorporated a means to measure the differential signal directly, whose details we will describe later on.

The "causal path" of mechanics for this problem is molecular adsorption → surface stress → deflection, i.e., the specific molecular adsorption "dictates" the surface stress, which "dictates" the cantilever deflection. Hence, the deflection can be directly calculated from the Stoney's equation given a surface stress associated with a specific biological activity occurring on the cantilever surface. Thus, we chose to design the cantilevers so as to handle various surface stresses that can result from different biological experiments, such as alkanethiol adsorption, pH detection and oligonucleotide or DNA hybridization.

Table 4.1 shows surface stress values, obtained from different biological experiments performed on various cantilevers. The resulting deflections, and, geometric and material properties of the cantilevers are also indicated.

Table 4.1. Summary of several surface stress sensing bio-experiments

Research Group	Berger	Fritz et al.	Wu et al.	Hai-Feng	MIT 6.151
Bio experiment	Alkanethiol adsorption	Oligonucleotide hybridization	Oligonucleotide hybridization	pH detection	
Tip deflection (nm)	200	10	30	400	9-900
Surface stress (N/m)	0.2	0.005			
Surface stress (N/m)	0.1	0.002	0.01	0.5	0.005-0.5
Beam material	Si3N4	Si	Si3N4	Si3N4	Si3N4
Young's Modulus (GPa)	150	166	180	270	270
Poisson's Ratio	0.23	**0.2**	0.25	0.27	0.27
Total beam length (um)	180	500	200	200	500
Effective length (um)	180	500	200	200	400
Beam thickness (um)	0.6	1	0.5	0.7	1
Beam width (um)	18	100	20	40	100
Density (kg/m^3)	3170	2331	3170	3170	3170
1st Natural freq. (kHz)	20.6	5.5	15.2	26.1	6.0
Gravity bending (nm)	0.000286	0.00554	0.000523	0.00018	0.00341
*Reported value					
*Senturia value					
***Senturia PolySi Value**					
*Length covered with molecules					
*Calculated value					

Although each of the above research groups used different cantilevers and concentrated on different biological activities, the mechanics of detection is fundamentally the same.

The oligonucleotide hybridization experiment of Fritz et. al. revealed a surface stress of $0.005Nm^{-1}$. Among all four experiments, this happens to be the lowest surface stress value. Though not reported by Hai-Feng et. al. [13], we calculated the surface stress of the cantilever used for pH detection to be $0.5Nm^{-1}$ using the Stoney's equation. In

accordance, we selected the geometrical parameters of our cantilevers, so as to accommodate surface stresses anywhere between $0.005Nm^{-1}$ and $0.5Nm^{-1}$, and result in tip deflections that are within the same order of magnitude as the values reported above. These parameters are on the rightmost column of Table 4.1. The effective beam length stands for the length of beam that is exposed to biological activity.
The difference in total length and effective length is the region that accommodates the interdigitated fingers for optical detection of beam deflection.

Although we will describe the fabrication procedure later on in detail, it is essential to mention some fabrication steps that influenced the design. We selected Si_3N_4 (Silicon nitride) as the cantilever material for simple and economic fabrication. Using single crystal silicon beams tend to require DRIE, which is an expensive process. However, Si_3N_4 beams can be released with a KOH etch, which is a simple and economic process that does not require a clean room. The choice of nitride on the other hand set an upper limit of $1\mu m$ on the cantilever thickness. This is because thicker nitride cantilevers tend to develop high stresses during fabrication and bare the risk of bending upon being released.

4.1.2 Interdigital Finger Design

The use of interdigital fingers as a displacement sensor was introduced by Yaralioglu et. al [16]. The method is based on optical interferometry. The geometry of the interdigital fingers forms a diffraction grating, which reflects an incident coherent optical beam into several orders. The intensity of each order depends on the spacing between the two sets of fingers, such as:

$$I_0 \propto \cos^2\left(\frac{2\pi}{\lambda}\xi\right) \tag{4.2}$$

and

$$I_1 \propto \sin^2\left(\frac{2\pi}{\lambda}\xi\right) \tag{4.3}$$

where I_o and I_1 represent the intensities of the zeroth and the first orders respectively. Also, λ and ξ here represent the wavelength of the incident beam and the relative displacement between the two sets of fingers, respectively.

Figure 4.1.1 shows the interdigital finger set that we designed for our cantilevers, where all dimensions are in microns. There are 6 sets of fingers. This is consistent with the recommendation of Yaralioglu et. al. [16] stating that the number of sets should be greater than 4 to ensure well separation of the diffraction orders. The length and width of each finger are

$70\mu m$ and $4\mu m$ respectively. The spacing between each finger is $2\mu m$. This design provides ample interferometry area to align a typical laser beam of $30\mu m$ diameter.

Figure 4.1.1. Interdigital finger pattern (dimensions in microns).

4.1.3 Combination of the cantilevers and the interdigital sensor

Figure 4.1.2 shows the device layout directly imported from the mask file. All dimensions are in microns. The device is shaped as shown so as to insert it easily into fluidic channels that will expose the cantilevers to bio-molecules. The short bumps on the very right and left of the device have been placed to prevent the liquid in the fluidic channels from contacting the interdigital fingers

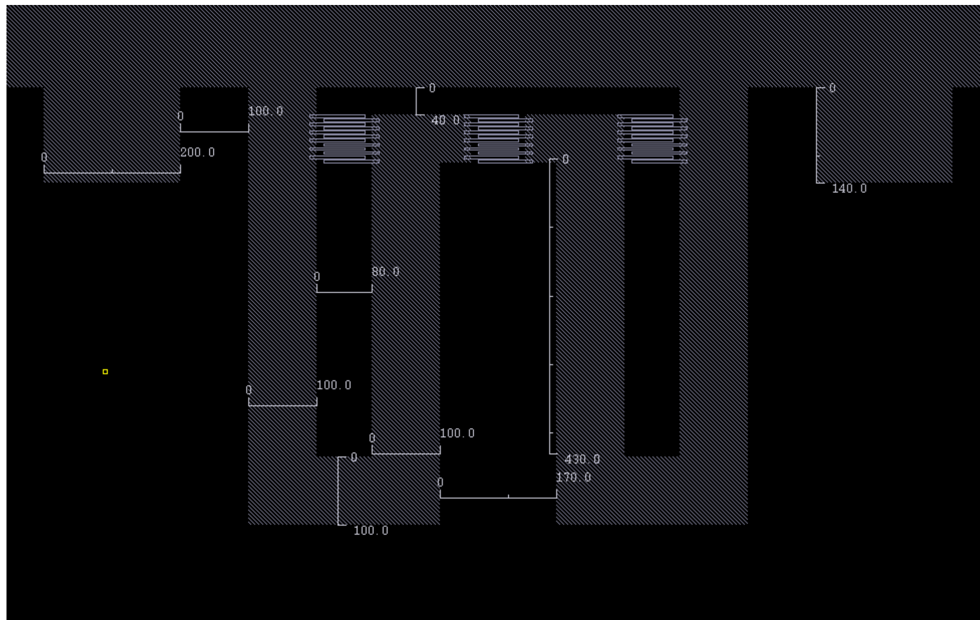

Figure 4.1.2. Top view of device (dimensions in microns).

The inner cantilevers are the sensors that bend in response to a surface stress. The outer cantilevers constitute the supports that connect the sensor cantilevers to the substrate. As we discussed in the high-level design section, these supports comprise the honeycomb structure. They are thicker (up to 8 times) than the sensor cantilevers, and experience negligible bending despite being exposed to bio-molecules.

Eventually, as we discussed in the high-level design section, the device surface will be covered with gold. This step is generally done immediately before the bio experiment. In order to ensure that the bio molecules (say DNA strands) bind onto the surface of the cantilevers, they are thio-modified. In other words, they contain sulphur at one end, and, sulphur forms a favorable bond with gold. It is this bond that facilitates the surface functionalization of cantilevers.

Although it is essential to get gold on the surface of the cantilevers, it is not desirable to expose the interdigital fingers to gold. This is because, the bio-molecules can adhere to the surface of the fingers and affect the reliability of the optical read out. Hence, the gold coating will have to be performed using a shadow mask that protects the interdigital fingers from gold exposure. For this reason, we designed the sensor cantilevers $30\mu m$ longer than the previously decided dimension of $400\mu m$. The gold coating step is beyond the scope of this report and no further detailed explanation about this step will be discussed here.
We will describe the fabrication of the device in the following section

4.2 Fabrication and Results

In this section, we describe the fabrication procedure, the difficulties that experienced during fabrication and the results obtained. The basics of the fabrication that define the cantilevers and the honeycomb structure are quite simple and illustrated in figure 4.2.1.

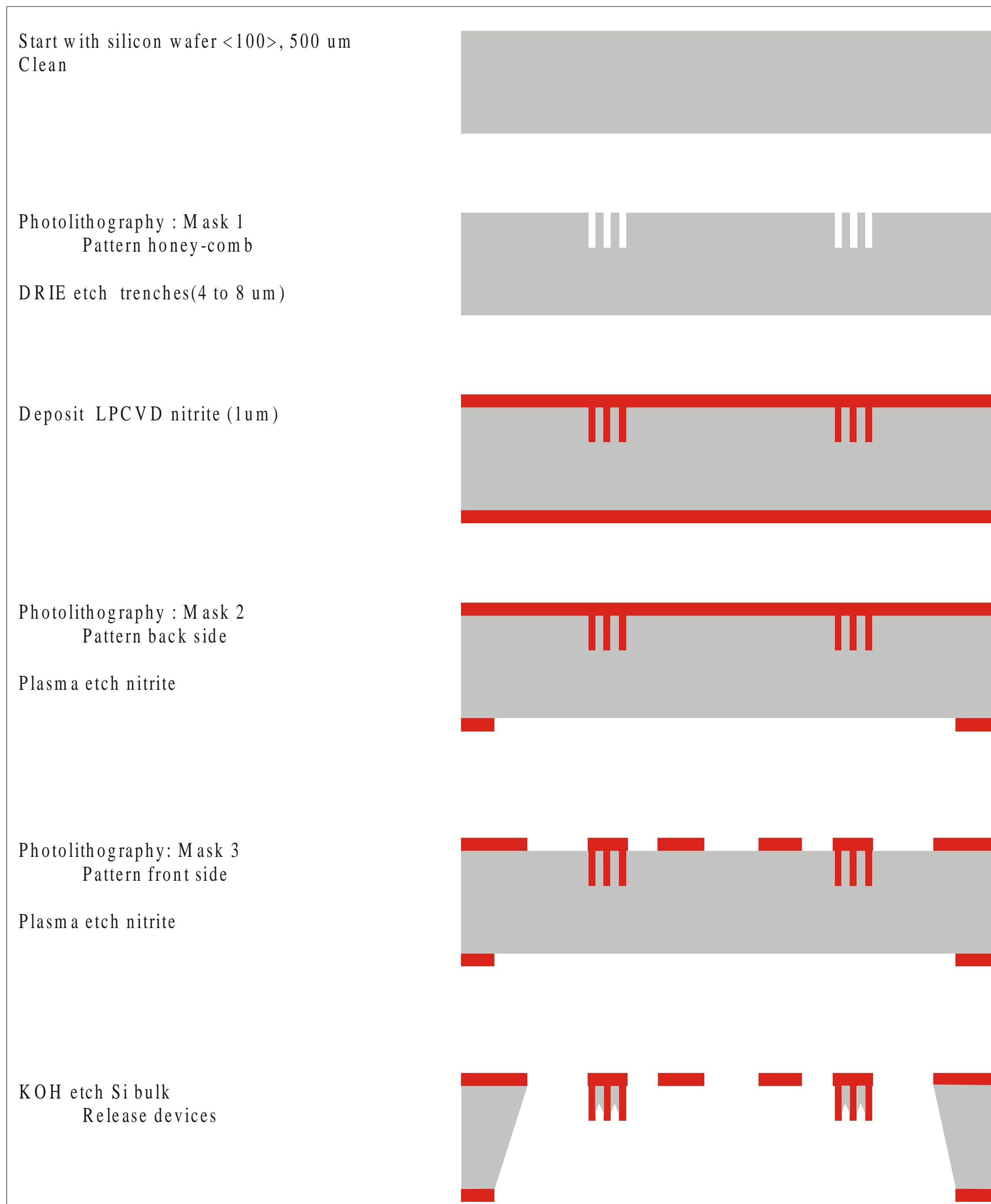

Figure 4.2.1. Basic fabrication steps of the double cantilever system

Figure 4.2.1 shows a cross-section of the device whose top view was illustrated in figure 4.1.2 of the design section. As we discussed in that section, the structures are constituted by nitride. Hence, the entire fabrication is based on depositing nitride on a silicon wafer and patterning it on both sides of the wafer to define the devices and the dies that accommodate them. The final step is to etch the silicon bulk in KOH and release the devices. The first main step is to pattern and etch the honeycomb. Here, it is important that the width of the honeycomb trenches be $2\mu m$ so that the trenches spontaneously

close when $1\mu m$ nitride is deposited. Here we pattern the nitride on the back side first, before defining the devices on the front side to eliminate the risk of damaging them. Another point of caution is to remember that KOH etch terminates on the <111> planes forming an angle of 54.7° with the horizontal. Back side mask (Mask 2) design takes this into account. This specific etch might also leave some silicon inside the honeycomb, but this is advantageous since the only purpose of the honeycomb is to provide stiffness.

Before we present the full process plan, we'd like to show the main features of the masks.

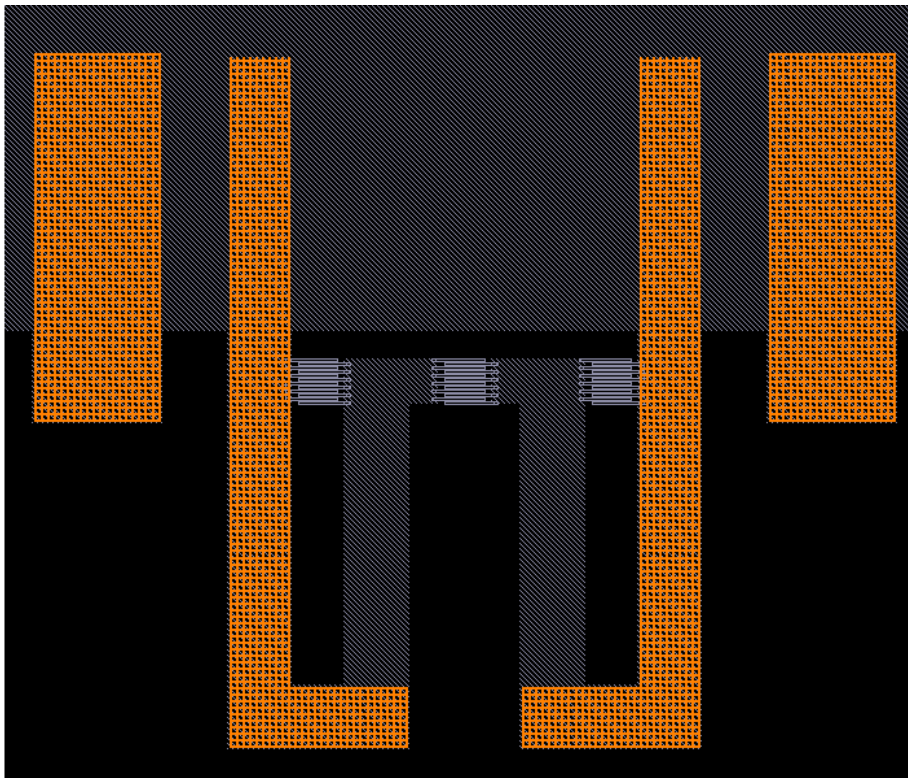

Figure 4.2.2. Superposition of Masks 1(honeycomb) and 3(device)

As we discussed before, the honeycomb structure provides support for the cantilevers and the bumps for fluidics insertion. This is also illustrated in figure 4.2.2, where orange color represents the honeycomb mask (Mask 1) and the gray shows the device mask (Mask 3). We would like to clarify that all masks for this fabrication process are dark field, i.e, orange lines of Mask 1 are in fact void. We asked the mask manufacturer (CompuGraphics) to take this fact into account.

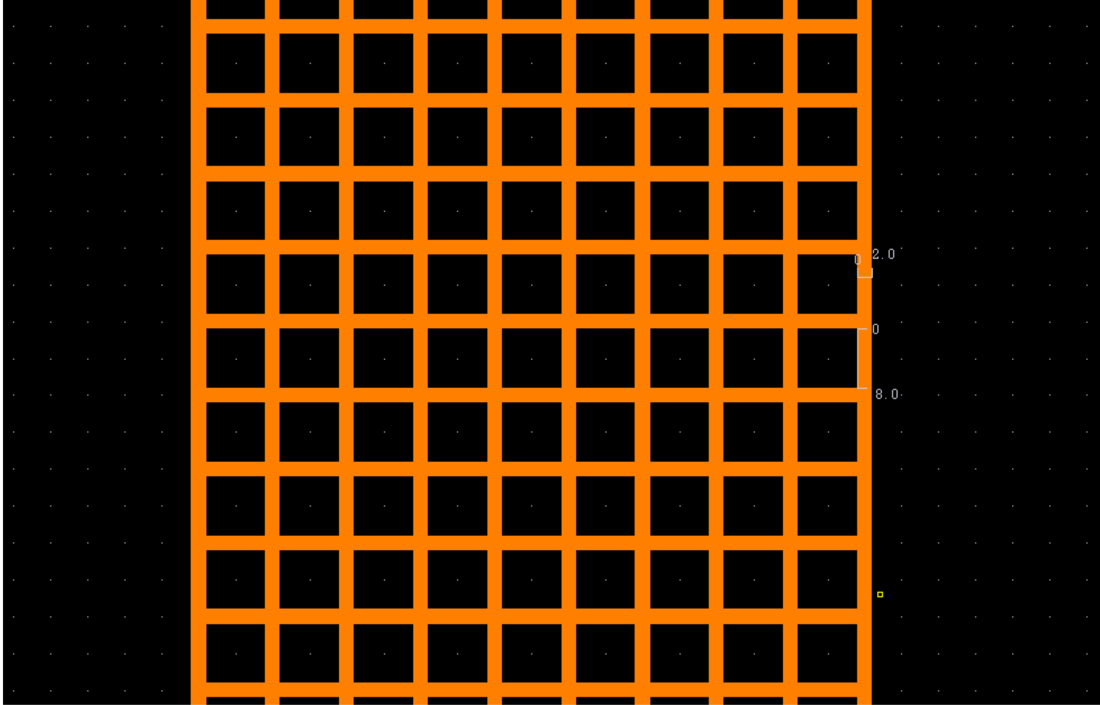

Figure 4.2.3. Detailed view of the honeycomb. (dimensions in microns).

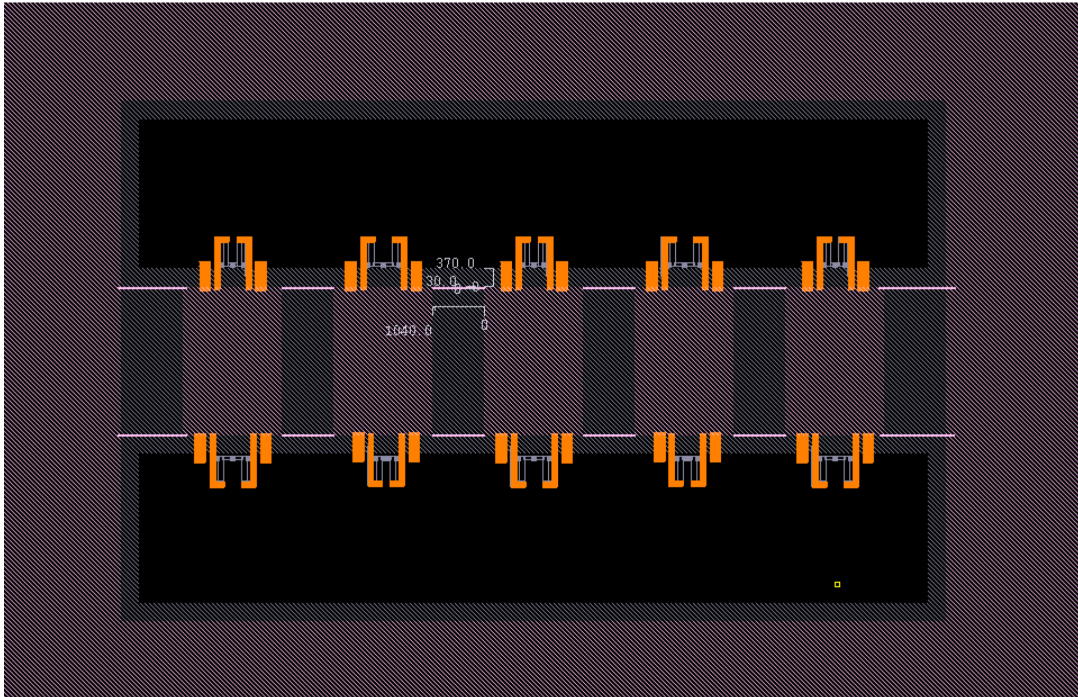

Figure 4.2.4. Superposition of all 3 masks (break-out unit of 5 dies) (dimensions in microns).

Figure 4.2.3 shows a section of the honeycomb mask in detail. We designed the masks so that 5 dies form a break-out unit. Figure 4.2.4 shows a break-out unit, in which each die has been assigned two different devices. The only difference between the two devices is the separation between the sensor cantilevers. We designed the additional device with the

larger separation ($370\mu m$) in case of possible difficulties in inserting the devices in fluidic channels. We alternated the devices in each row, in order not to loose all devices of the same kind, in case of a mishap that occurs on one side of the break-out unit.

The purple color in figure 4.2.4 is Mask 2, which is used to pattern the back side of the wafer to define the bottom of the dies, and, at the same time the etch mask for KOH. We connected the dies with break-out tabs that are $1040\mu m$ long and $30\mu m$ wide. Since the final etch is in KOH, a space of $1040\mu m$ between dies at the bottom of the wafer will result in a gap of only $300\mu m$ at the top side (assuming a wafer thickness of $520\mu m$). The same phenomenon is responsible for the $370\mu m$ space that we left between the edges of Mask 2 and Mask 3.

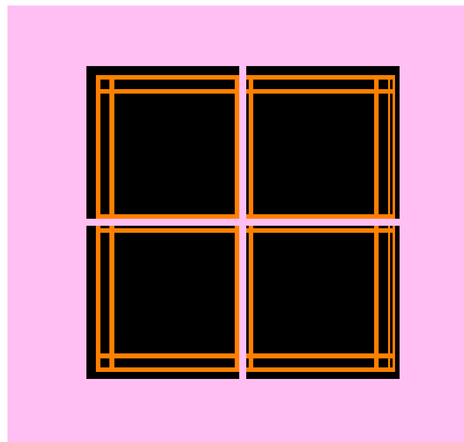

Figure 4.2.5 Alignment features of Masks 1 and 2.

Figure 4.2.5 shows how the backside mask is aligned between the $2\mu m$ wide trenches formed by the honeycomb mask (Mask 1). The color of Mask 2 was intentionally changed from what it was in figure 4.2.4 to clarify the cross, which has the primary dimension of $210\mu m$.

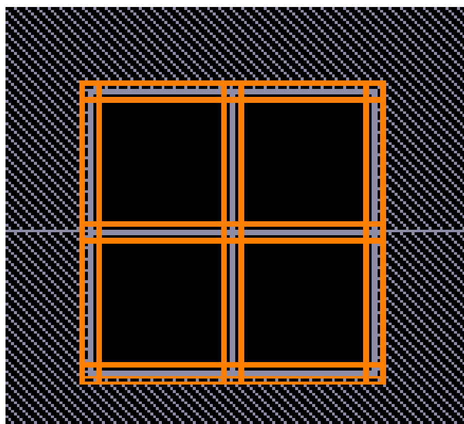

Figure 4.2.6 Alignment features of Masks 1 and 3.

Figure 4.2.6 shows the alignment of the device mask between the $2\mu m$ wide trenches formed by the STS etch.

We now introduce the full process plan and describe the results of the fabrication.

Table 4.2. Full process plan on 4'' double-side polished Silicon wafer <100>, 525um

Step#	Lab	Machine	Recipe	Description
1	ICL	Pre-metal	Piranha clean	
2	TRL	HMDS	HMDS	~25 Å
3	TRL	Coater	1um	Coat 1um positive P.R
4	TRL	Prebake oven	90ºC, 30min	Pre bake
5	TRL	EV1	~1.5 s	Exposure, Mask #1
6	TRL	Photo-Wet-l	1 ~ 2min	Develop P.R
7	TRL	Postbake	30 min	Post bake
8	ICL	STS	20um Shallow Etch	Etch Silicon trenches (up to 8um)
9	TRL	RCA station	Brown-dot RCA	Cleaning for VTR
10	TRL	Oxidize tube	O2 1100ºC, 30 min	Remove STS residue
11	TRL	Acid-hood	BOE	Remove oxide
12	TRL	RCA station	Brown-dot RCA	Cleaning for VTR
13	ICL	VTR	~ 7 hrs	Deposit on both sides: 1um, 10:1 Si rich, low stress SiNx by LPCVD
14	TRL	HMDS	HMDS	~25 Å
15	TRL	Coater	1um PR	Frontside protection layer
16	TRL	Prebake oven	90ºC, 5 min	Prebake PR
		Invert Wafer (to back side)		
17	TRL	Coater	1um	Coat 1um positive P.R
18	TRL	Prebake oven	90ºC, 30 min	Pre bake
19	TRL	EV1	1.5 s	Exposure, Mask #2
20	TRL	Photo-Wet-l	1 ~ 2 min	Develop P.R
21	TRL	Postbake	30 min	Post bake
22	ICL	AME5000	CF4, 400 s	Etch SiNx
23	TRL	Acid-hood	Piranha Clean	Strip P.R
		Invert Wafer (to front side)		
24	TRL	HMDS	HMDS	~25 Å
25	TRL	Coater	4.5um	Coat 4.5um positive P.R
26	TRL	Prebake oven	90ºC, 30min	Pre bake to harden PR
27	TRL	EV1	1.5s	Exposure, Mask #3
28	TRL	Photo-Wet-l	1~2 min	Develop P.R
29	TRL	Postbake	30 min	Post bake
30	ICL	AME5000	CF4, 360 s	Etch SiNx
31	TRL	Acid-hood	Piranha Clean	Strip P.R
32	TRL	Acid-hood	BOE	Strip native SiO2, use water to check
33	Media Lab	KOH	60ºC, 25%KOH, ~ 10hrs	Etch Silicon, release devices

We experienced the first difficulty during photolithography with Mask 1 (steps 3 through 5). We first anticipated photoresist failure in STS and coated $7\mu m$ thick resist. This however resulted in poor photolithography, i.e., we obtained honeycomb trench patterns that were wider than $2\mu m$. We concluded that this was because of some of the light getting trapped in the resist, as opposed to being reflected straight back out through the opening of the mask. As a result, more resist coming off during the development than we planned. A honeycomb trench that is wider than $2\mu m$ is not desirable since a $1\mu m$ thick LPCVD nitride would not close the trench and result in problems in the future when we try to coat this side with photoresist. It might also cause problems during the final KOH etch if the nitride deposition is not sufficiently uniform. Since we discovered our mistake before putting the wafer in STS for step 8, we stripped off all photoresist with piranha and repeated this step with $1\mu m$ thick photoresist. The result of the photolithography appeared satisfactory under the microscope, hence we proceeded with DRIE.

We initially planned on making the honeycomb trenches $20\mu m$ deep. However, later on we were afraid that the nitride deposition may not be uniform due to the high aspect ratio. Hence, we decided to reduce the depth. However, the recipe that we used with the STS was "$20\mu m$ shallow etch", and the depth of a trench below $20\mu m$ was not guaranteed. Despite this risk, we etched 2 wafers, one for 2 minutes, and one for 4 minutes, assuming an etch rate of $1\mu m$ per minute.

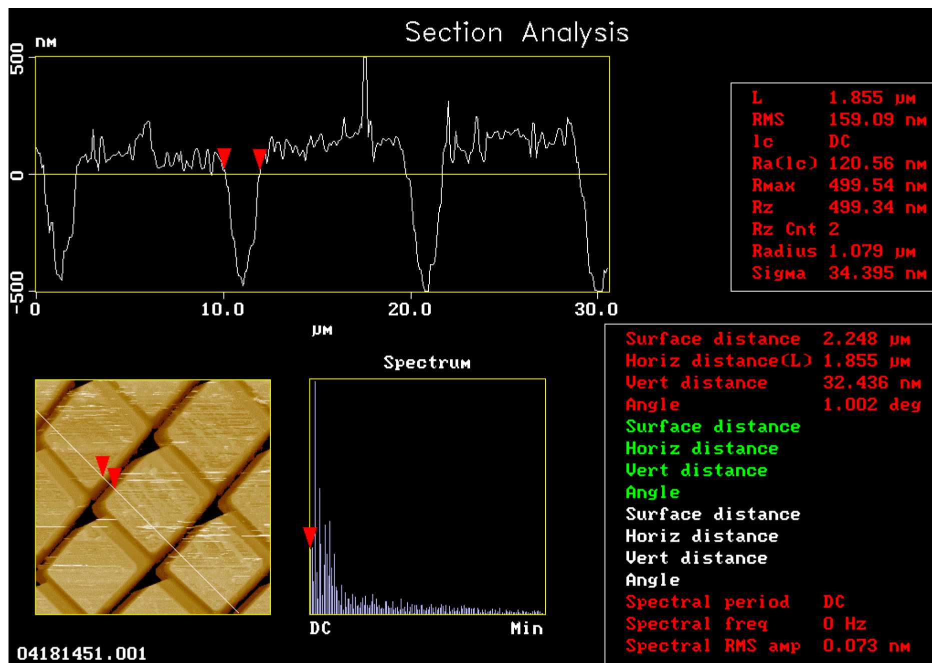

Figure 4.2.7 AFM image of a test wafer after the STS etch .

Figure 4.2.7 shows an AFM image of the honeycomb pattern of a test wafer that was etched for 4 minutes in the STS. The width of a honeycomb trench appears to be $1.855\mu m$ which compares quite well with the $2\mu m$ target width. The depth profile on top of the figure is ambiguous since the stroke of the piezoelectric actuators that operate the tip of the AFM is too small to measure a depth as large as $4\mu m$. Hence, we performed an optical test on the same wafer to detect the depth of the trenches.

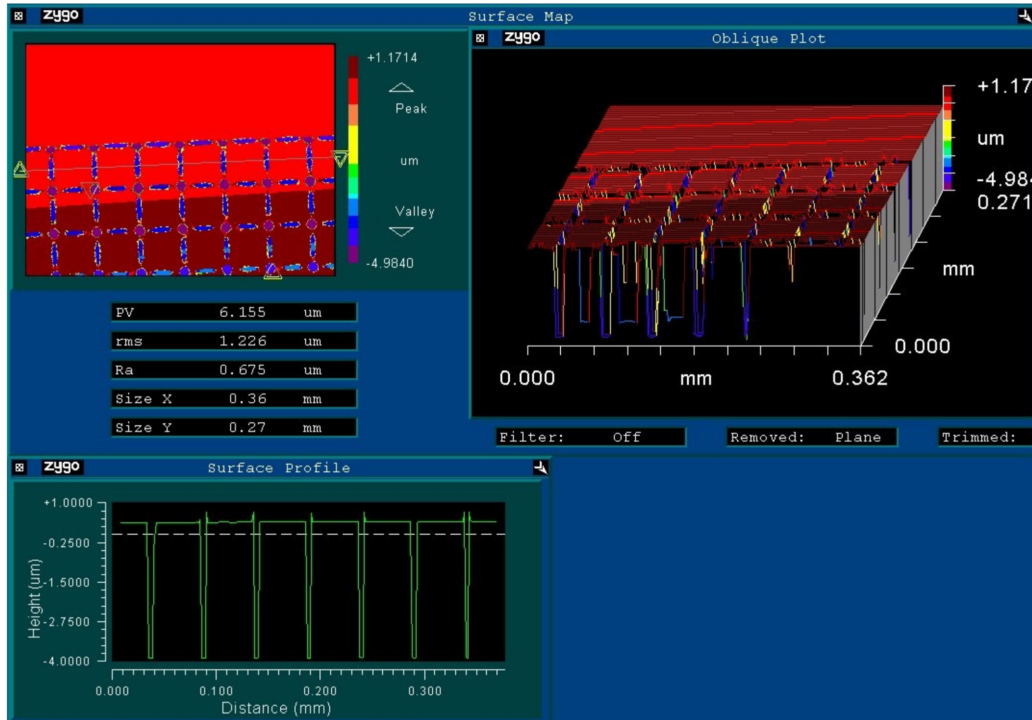

Figure 4.2.8. Zygo Image of a test wafer after STS etch.

Figure 4.2.8 shows the results of an optical test performed with a Zygo machine. The depth appears to be almost exactly $4\mu m$. Feeling confident with the results, we decided not to perform the same measurements on the wafer that was etched for 2 minutes and assumed that the depth of the trenches on that wafer were exactly $2\mu m$. Feeling confident about the results of the STS etch, we proceeded with the cleaning procedure for VTR.

In MTL, wafers are not allowed in VTR if they had been in STS. The reason is that STS coats the sidewalls of the trenches with a teflon passivation layer to prevent the SF_6 etch from progressing sideways, and, teflon causes a non-trivial contamination in VTR. Thus we proceeded with a set of steps (9 through 12) which was previously approved by MTL.

These steps comprise growing a thin layer of oxide on the trenches, and burning the teflon. The BOE etch then removes the oxide along with the teflon. A final RCA is necessary before a wafer is introduced in VTR.

LPCVD $1\mu m$ silicon rich nitride was deposited in VTR for a period of approximately 7 hours. Silicon rich nitride was necessary to ensure low stress, and hence, to prevent the beams from bending after release. Thickness measurements indicated 10050A which was almost perfect.
We then inverted the wafer and proceeded with the back side patterning with Mask 2. We had to align this mask to the features defined by Mask 1 on the other side of the wafer. Finding alignment features was quite difficult, because it turned out that our alignment features were not large enough. In addition, they were too far away from other features. Yet, it was still possible to perform the alignment with considerable accuracy.

The proceeding plasma etch in AME resulted in resist failure. We confirmed this by measuring the thickness of the nitride on the back side to be 6000A. A nitride layer with this thickness is acceptable for the back side provided that it withstands the long KOH etch, since the only purpose of the back side patterning is to define the dies and form an appropriate etch mask for KOH. We confirmed this by etching a test wafer in KOH for approximately 17 hours and observing that the back side nitride was able to withstand the KOH.

This thickness however is not acceptable for the front side, since the front side nitride constitutes the devices, which we have designed to be $1\mu m$. Hence, to protect the $1\mu m$ thick nitride layer, we decided to use thicker resist while patterning the front side with Mask 3. We coated one wafer (with $2\mu m$ deep honeycomb trenches) with $4.5\mu m$ thick resist and another wafer (with $4\mu m$ deep honeycomb trenches) two times with $1\mu m$ thick resist. We had similar difficulties in finding the alignment features, but alignment itself was eventually successful. Investigations of both wafers under microscope, following development showed that double coating to achieve $2\mu m$ thick resist was a better method than using $4.5\mu m$ thick resist. The features (interdigital fingers) on the wafer with thicker resist seemed to be slightly thinner than expected, however, the results were still acceptable. Hence, we proceeded with the AME etch. Coating the front side with a resist thicker than $1\mu m$ was correct: The resist was still attacked by the AME, but not enough to allow let the protected nitride layer to start eroding. The thickness of the nitride that constitutes the devices was measured to be $1\mu m$.

Due to time constraints, we only etched one wafer (with $2\mu m$ deep honeycomb trenches) in KOH. The etch took about 10 hours, as opposed to 17 hour which is how long it took with the test wafer. We concluded that this was because KOH had attacked the wafer from both sides. The following figures show various optical and SEM images of a device.

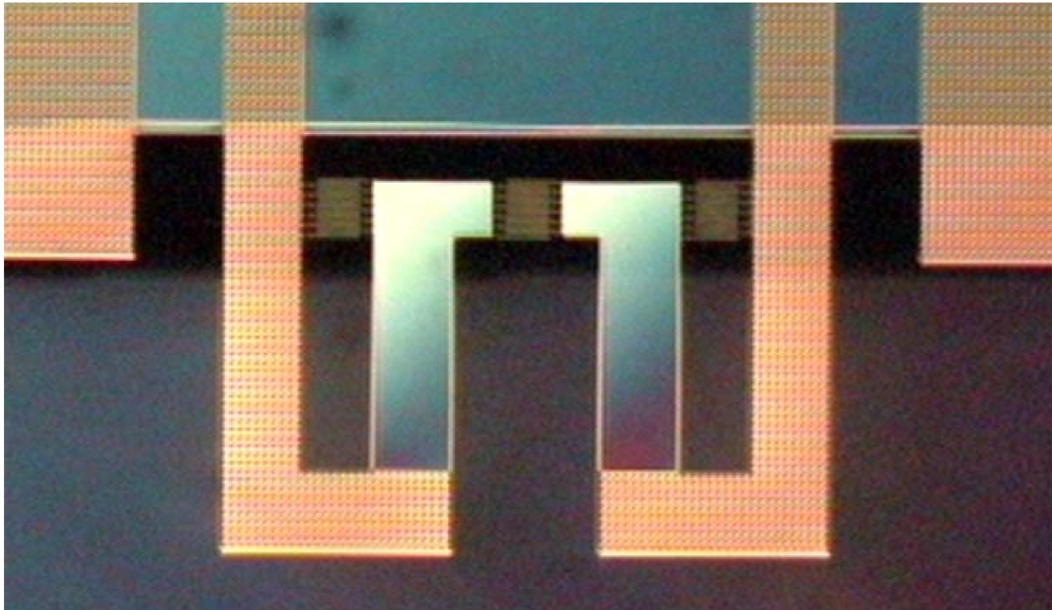

Figure 4.2.9. Top view of a device after KOH etch

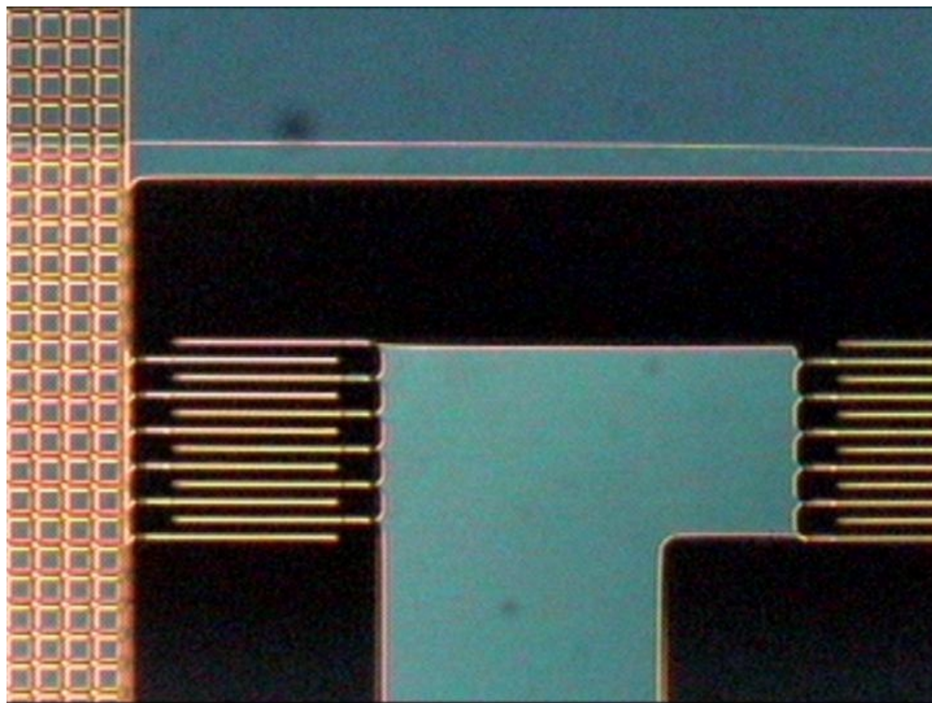

Figure 4.2.10 Interdigital fingers after KOH etch

Figure 4.2.10 shows a detailed view of the interdigital fingers and the honeycomb. We clearly observe the nitride layer on the cantilever and the substrate. The honeycomb and the fingers, although being nitride have assumed a different color. We believe this is because of the relatively small size of the honeycomb trenches and the fingers. As we discussed before, the fingers are thinner than expected. This is because of the thick resist that was used during the photolithography step. We believe that the other wafer that patterned using double coated thin resist will reveal more accurate finger geometry.

Figure 4.2.11. SEM view of the (honeycomb support)-(sensor cantilever) junction

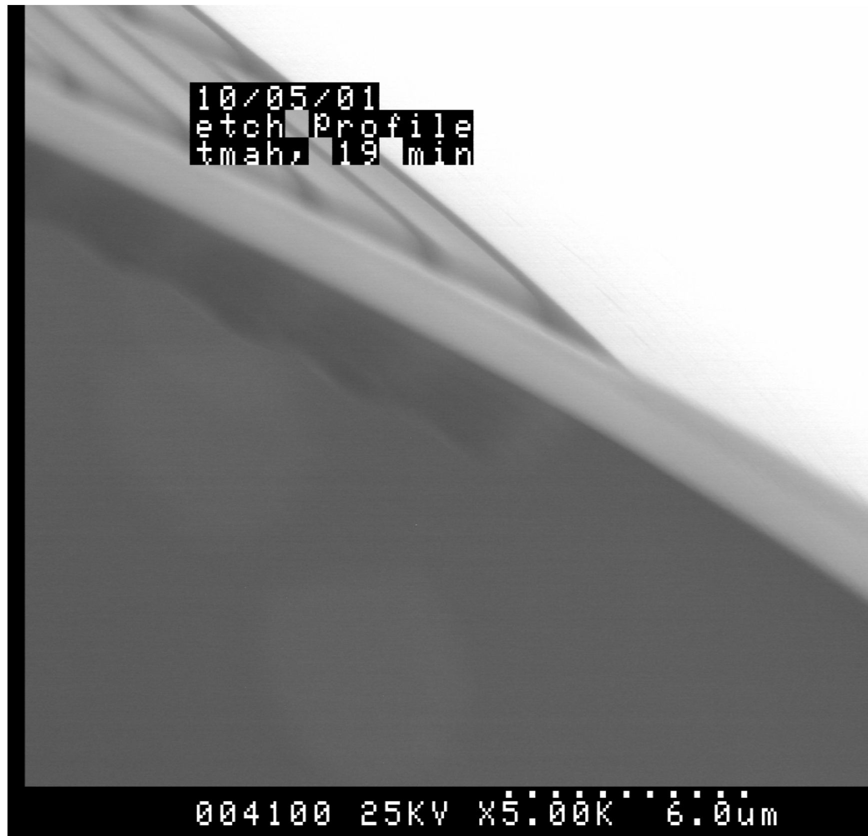

Figure 4.2.12. SEM side view of honeycomb structure

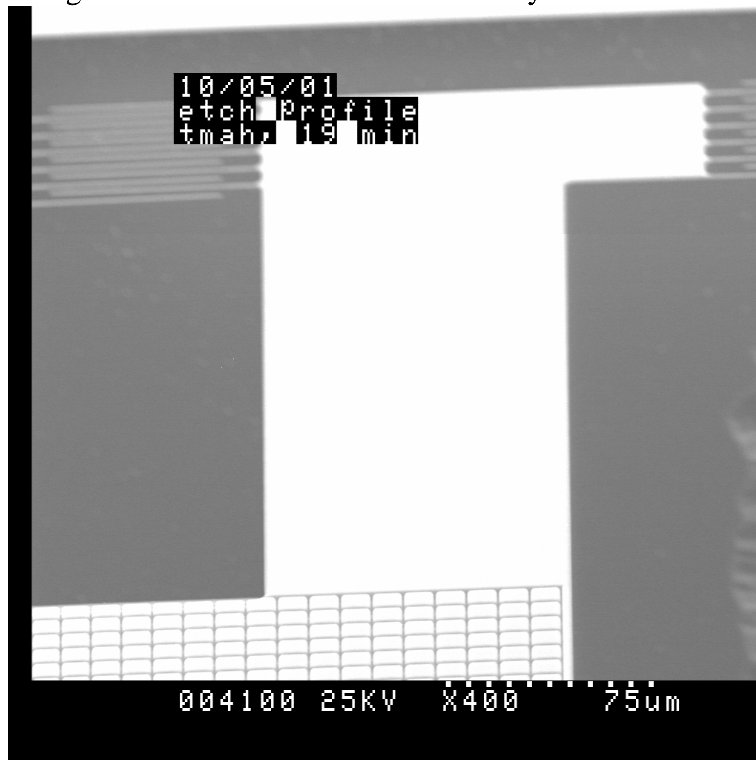

Figure 4.2.13 SEM of device

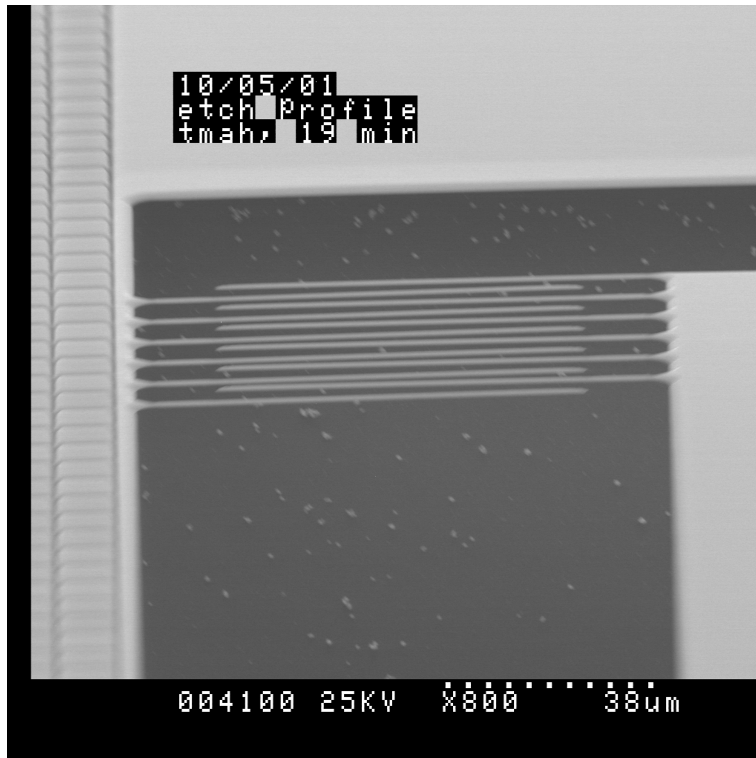

Figure 4.2.14. SEM of interdigital fingers.

Figures 4.2.11 through 14 are various SEM images taken after coating the surface of a device die with gold. These images provide details on sides of structures that optical views lack. Figure 4.2.12 confirms that the honeycomb structure is almost exactly 2 times as thick as the $1\mu m$ thick cantilever.

4.3 Recommendations and Conclusions

We designed and fabricated an interferometric bio-sensor using conventional microfabrication techniques, over a period of one academic semester. We believe our results indicate that our process plan was well-thought and carefully followed through. In this section, we briefly discuss some conclusions and issues that can facilitate a future work for fabricating a similar device.

STS is a powerful tool in achieving high-aspect-ratio trenches. We also believe that the accuracy of the "$20\mu m$ shallow etch" recipe for trenches that are shallower than $20\mu m$ is underestimated. However, we did not test the repeatability of this recipe, hence, we will not draw conclusions. We only say here that the etch rate of this recipe was almost exactly $1\mu m$ per minute, during the fabrication of our honeycomb trenches.

During the course of fabrication, we repeatedly observed that thin resist results in more accurate feature dimensions, than thick resist. However, it is not possible to conclude that the resist used must be as thin as possible, since this depends on what kind of an etch follows the photolithography step and how selective this etch is in consuming photoresist.

For our case, it is certain that the CF_4 gas used by AME to etch nitride consumes photoresist. Although a thorough study for quantification of this consumption would be helpful, we believe that it is in the best interest of the research team to coat sufficiently thin resist and perform an etch with a test wafer immediately before etching the device wafer. We reached this conclusion based on interactions with several technicians and research assistants, who stated that the resist consumption level could vary depending on the process history of the machine within that day.

Another aspect of AME is that it does not perform a uniform etch. The mid sections of the wafer get etched quicker. Therefore, it is necessary to take this into account while selecting the etch time.

We would also like to mention that the cleaning process for the “STS-to-VTR transition wafers” has proven useful and could be applied with relative confidence in the future.

One point of caution for mask design is that it is not a good idea to place alignment features too far away from device features. This makes it quite difficult to find them during actual alignment.

Our final recommendation is on the more practical side. It is necessary that the fabrication team list the machines to be used, and contact the corresponding technicians as early as possible. This way, all trainings can be completed in a timely fashion and delays in the actual fabrication run can be prevented.

5 MICROCHANNEL DESIGN & FABRICATION

5.1 Design

Cantilever functionalization is a multi-step process that prepares the cantilever surfaces for DNA adhesion. This is described in detailed in Fritz's paper [1], and is summarized below:

1. E-beam evaporate 1nm of Ti & 20nm of Au.
2. Coat one cantilever with hexadecanethiol (HDT).
3. Coat the other with mercaptohexadecanoic acid (MHA) or a combination of HDT and MHA. HDT and MHA can be dissolved in solution with ethanol to form a carrier liquid.
4. Rinse cantilevers in ethanol and dry.

To coat the cantilevers with HDT or MHA we decided to fabricate micro channels to convey the carrier liquids directly to each cantilever.

The microfluidic channels are made by first spinning on SU-8 (>100mm) ([5],[22]) on the silicon wafer, then patterning in shape of channels, followed by casting PDMS, and finally aligning and sealing the channels on another piece of material. SU-8 is a chemically resistant, negative photoresist that can form high-aspect ratio structures; PDMS (polydimethylsiloxane) is a transparent moldable elastomer, which is chemically unreactive, hydrophobic, and it can be irreversibly bonded to itself, glass, or silicon after plasma treatment . A variety of PDMS-based MEMS have been fabricated for biomedical or other uses ([18],[19],[20]). These devices are inexpensive, disposable, and easily made with access to a Class 10,000 clean room; the features can be as small as 25mm; and the moving fluid inside the channels can be either syringe pumped, or with metal electrodes formed within the device, electropotentially driven.

We had the following **design requirements:**

- The carrier liquids must be delivered directly to each cantilever without mixing, such that only one cantilever is coated by a particular carrier liquid.
- Each cantilever should be coated as fully as possible--this is made easy by the attraction of the thiols to Au and surface tension.
- The cantilevers should be subjected to as little stress as possible during coating.
- The interdigitated fingers should not be coated.

We chose the following design:

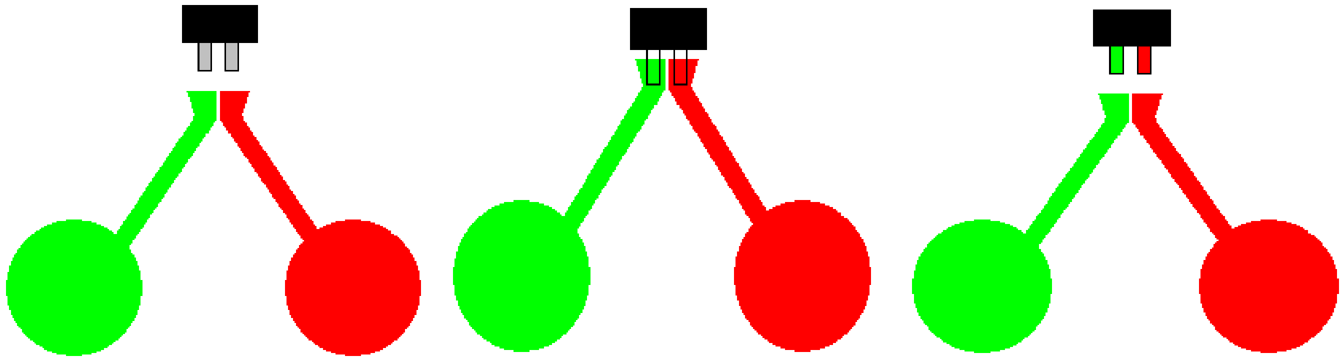

Figure 5.1.1. Schematic of the working principle

with specific design features and dimensions:

8220um
2300um
3822um
2445um
3830um
fluid rersevoir
475um
50um
675um
570um
fluid spout
magnified for clarity

Figure 5.1.2. Mask for SU-8 lithography

Design features:

- The double-spout arrangement allows for insertion & coating of both cantilevers simultaneously.

- The outer walls of the spouts are angled outwards. This was done to offset the concavity arising from the surface tension of a wetting liquid. It is hoped that this will cause surface of the liquid will be more flush with the mouth of the spout so that the cantilevers will be able to easily reach the liquid surface upon insertion (see fig 5.1.3).

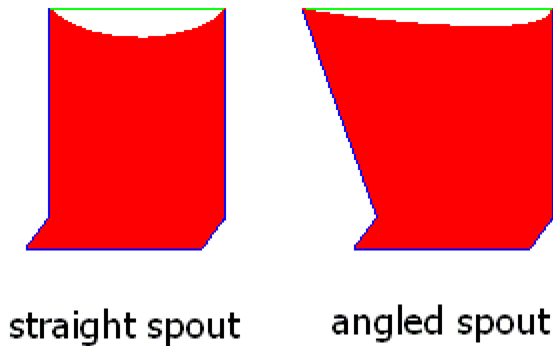

- The inter-channel spacing is thin only near the spout (shown as "d" in figure 5.1.2.) for ease of alignement with cantilevers, widening as the channel approaches the reservoirs. This was done so that the PDMS wall will have enough surface area to bond to the glass surface for the length of the channel from reservoir to spout, thus avoid leakage between the two channels.
- There is a macroscopically large cavity capping the spouts, included to make alignment to the edge of the glass slide easier. And as shown in figure 5.1.4, a simple cut along a straight line outside the spout can open the spouts without hurting the delicate structure around them.

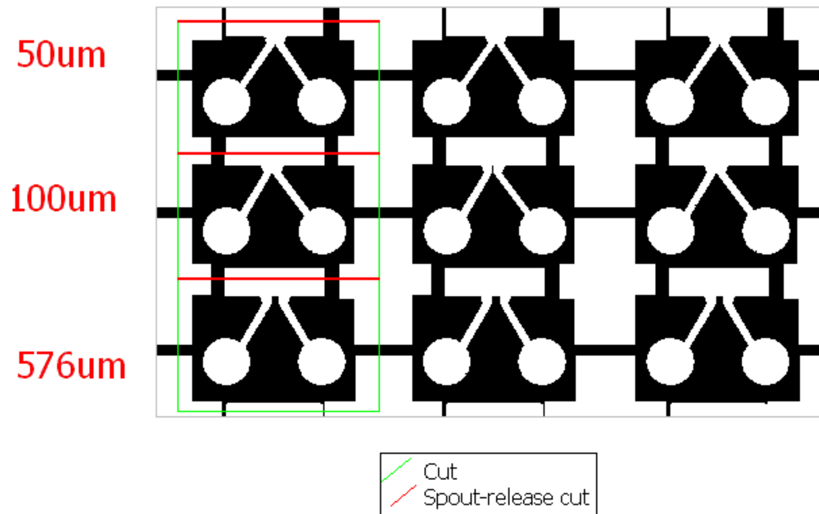

Figure 5.1.4. Dicing of the PDMS mold

- The reservoirs were designed to be macroscopically large so that it would be possible to aim the medical coring syringe without the aid of a microscope.

5.2 Fabrication and Results

Fabrication of the microfluidic channels was done both in the EML clean room of the MTL and the Nanoscale Fabrication laboratory of the Media Lab. A detailed summary of the process including the mask making can be found in the appendix. A graphic overview of the process is included as Figure 5.2.1.

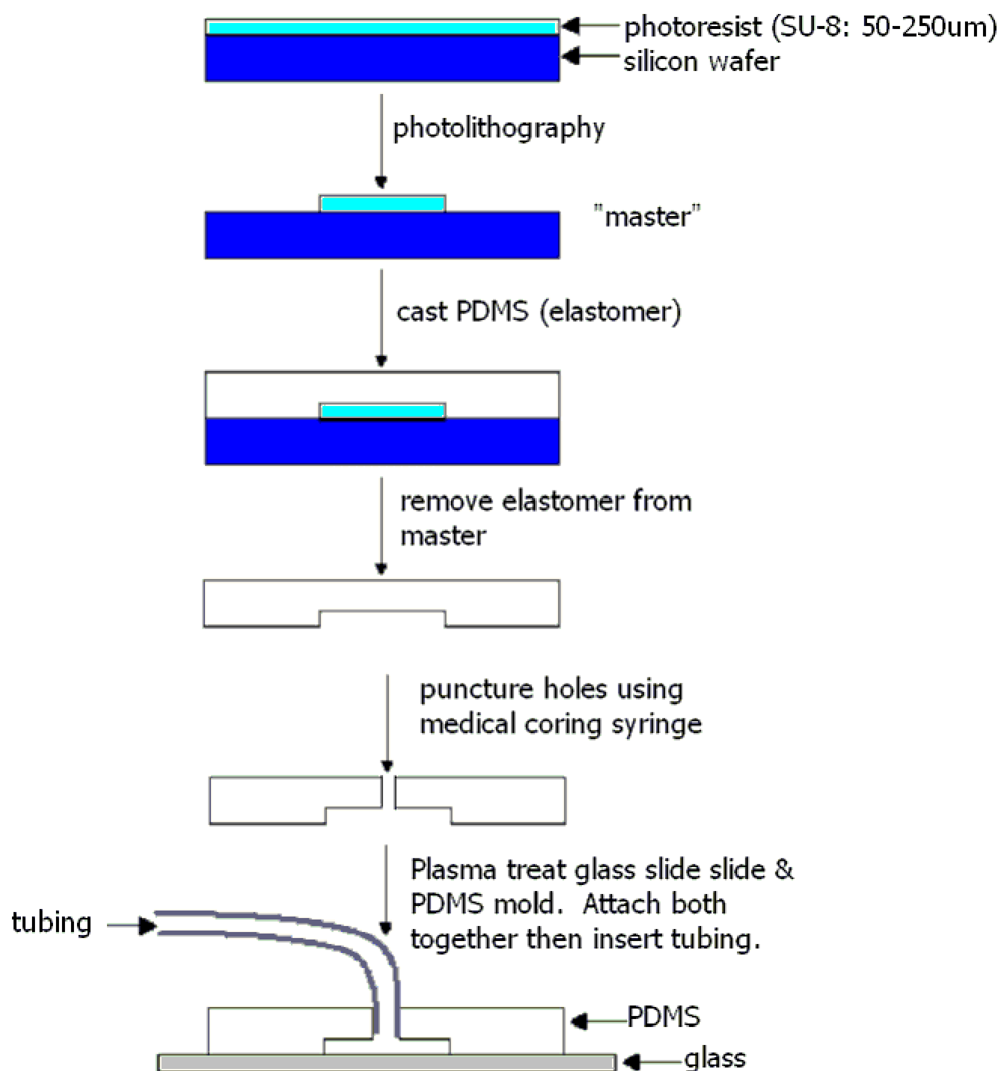

Figure 5.2.1 Overview of the Fabrication Procedure

Process flow

1. **Fabrication of Transparency Mask**

1.1 Design mask in Macromedia Freehand 9.0

1.2 Submit to Pageworks allow 1 day for delivery

2. **Fabrication of Silicon Master**

2.1 Piranha clean silicon wafer (we used clean wafer and didn't take this step)

2.2 Dehydrate silicon wafer on hotplate at 200 C for 20 min

2.3 Spin coat SU-8 – start at 500 rpm for 10 s and increase to 3000 rpm for a total of 30s

2.4 Prebake SU-8 on hotplate – ramp temperature from RT to 105 C, hold at 105 C for 15 min, allow to cool to RT

2.5 Expose resist for 2 min through transparency mask

2.6 Post-bake resist on hotplate (same schedule as for prebake at 1.4)

2.7 Develop resist in PGMEA

2.8 Place wafer in vacuum dessicator for 2 hrs with silanizing agent.

3. **Fabrication of Fluidic Channels**

3.1 Mix PDMS prepolymer components (10:1) and degas under vacuum

3.2 Pour prepoymer over silicon master in petri dish

3.3 Cure PDMS in oven at 90 C for about 1 hr

3.4 Remove PDMS fluidic channels from master

4. **Device Assembly**

4.1 Clean PDMS with tape.

4.2 Place both slides and PDMS channels into asher and treat with air plasma for 60s, HIGH setting.

4.3 Assemble the slides and PDMS by pressing them together

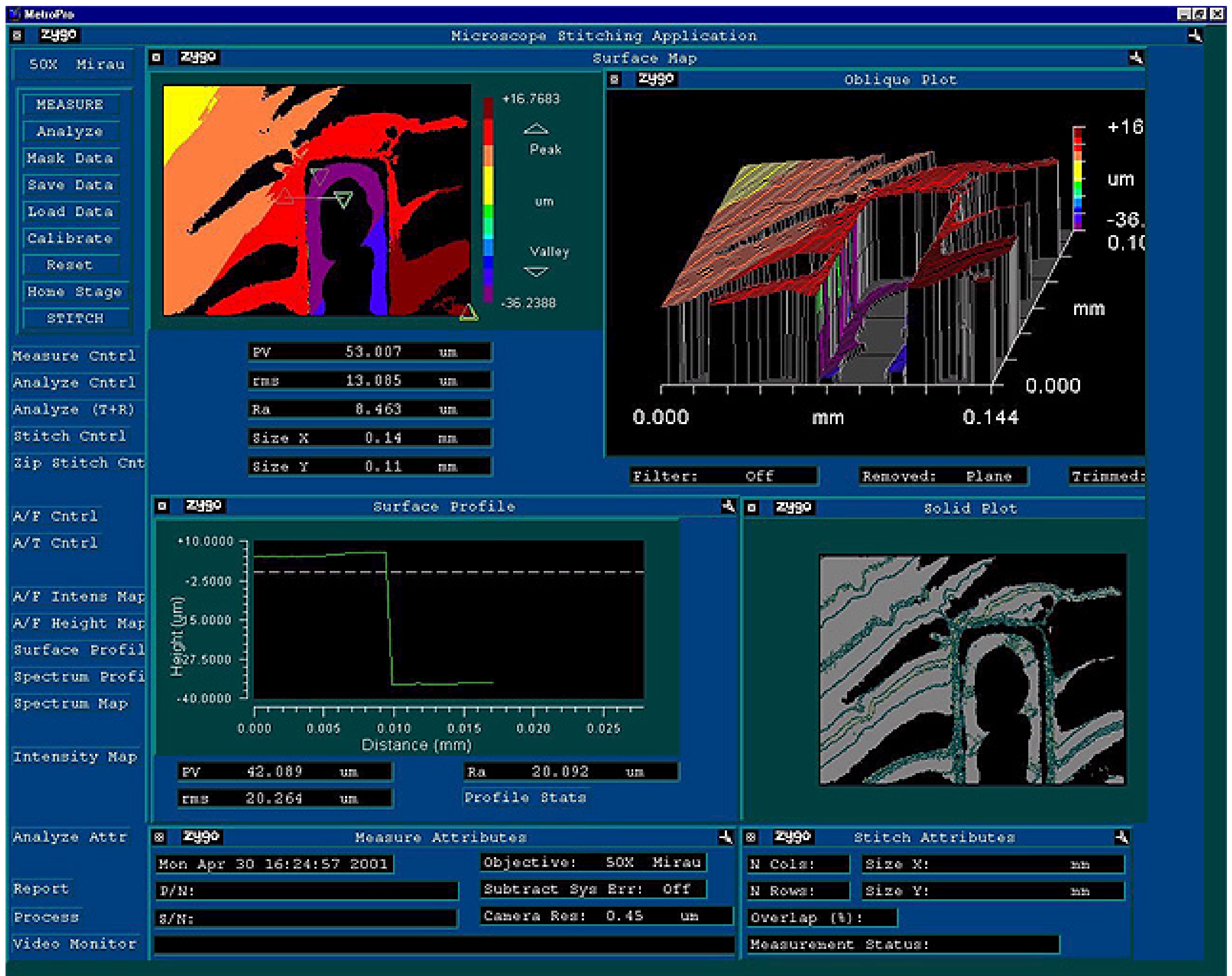

Figure 5.2.2. Topography of the master wafer obtained with an optical profilometer

Figure 5.2.2. shows a picture of one of the master wafers taken with an optical profilometer. With proper arrangement, 30 complete devices can be made on one wafer. In our design, three differently sized devices were made on the same wafer (see Figure 5.2.3).

The SU-8 master and PDMS cast obtained are shown in figure 5.2.3.

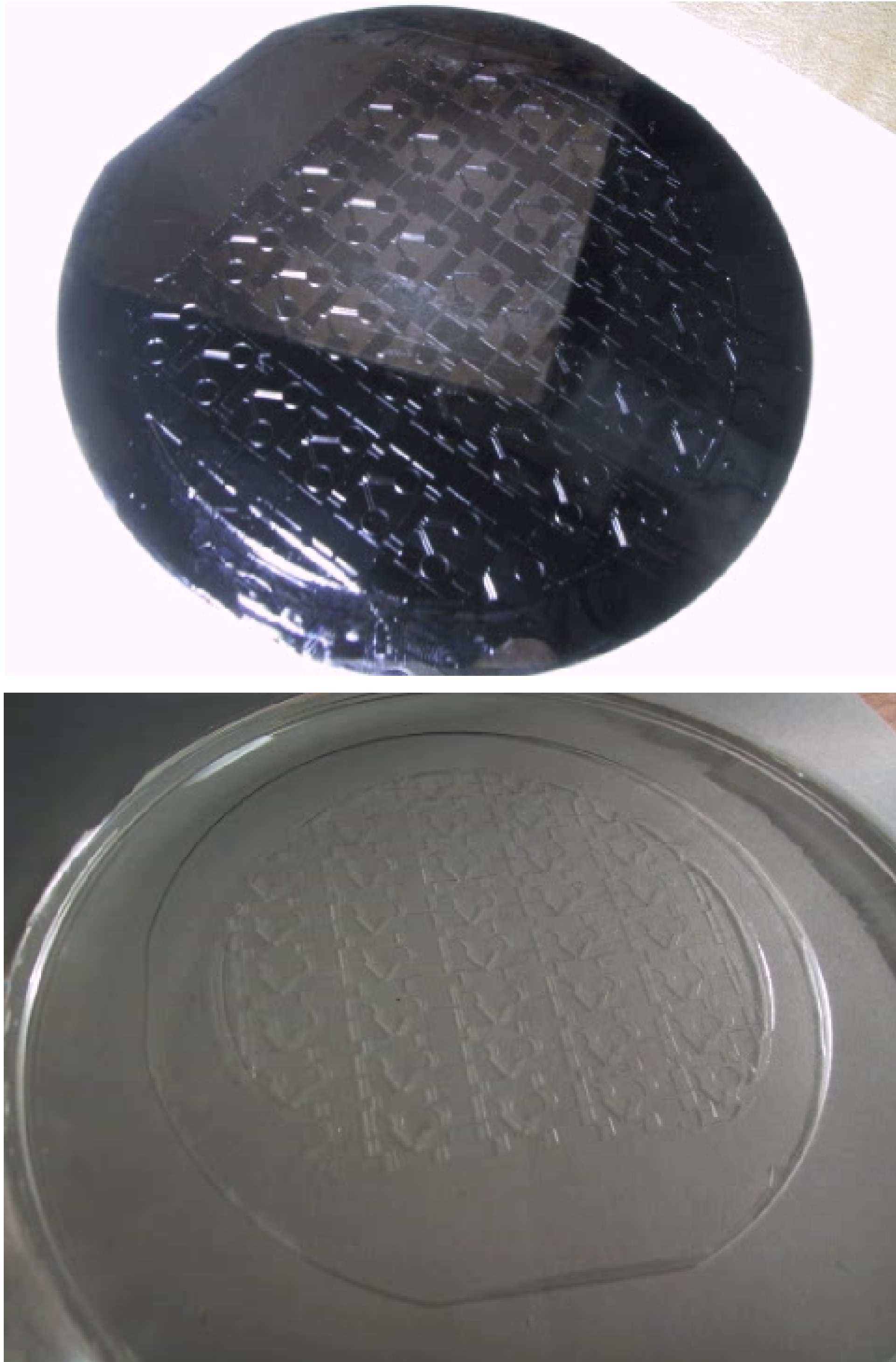

Figure 5.2.3. SU-8 master and PDMS cast

Under the microscope, the fine structure of the fluid channels in the PDMS can be investigated. Figure 5.2.4. shows both the section around the spouts (upper) and the connection from the reservoir to the channel (lower). The channel walls turned out fairly smooth.

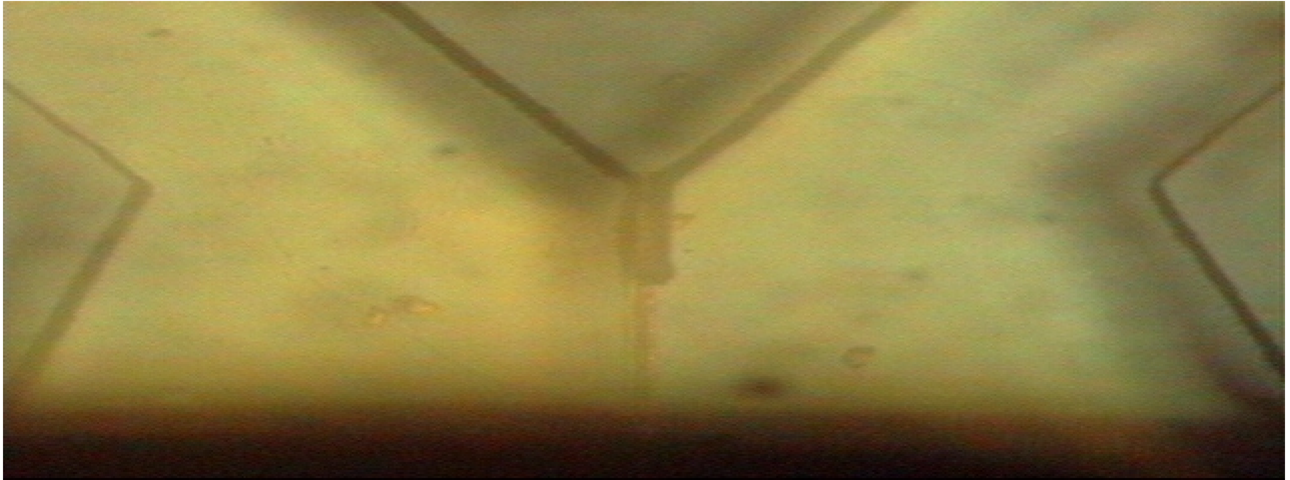

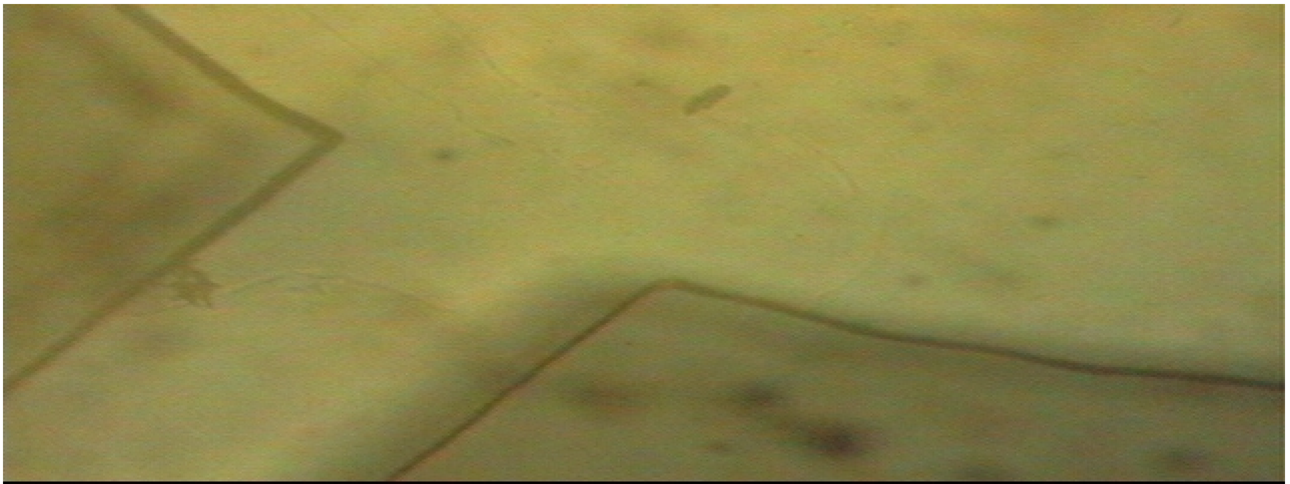

Figure 5.2.4.: Microscope pictures of the molded PDMS

A single fluidic device was finished by dicing the PDMS mold and bonding it to a glass slide in order to close the fluid channels. Tubing was connected to the reservoirs as shown in Figure 5.2.5.

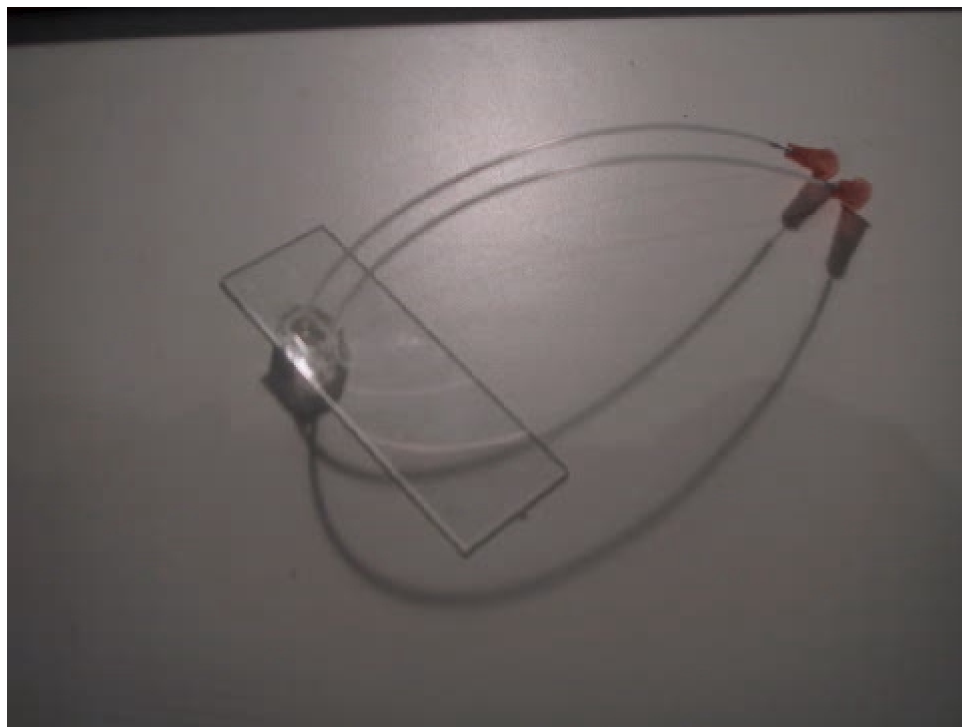

Figure 5.2.5. Device attached to a glass plate and equipped with tubing

Using an electronically controlled syringe pump, the reservoirs in the device can be filled with the desired fluid (Figure 5.2.6). The micro cantilevers were fixed on a glass plate opposite the micro channel device for alignment testing.

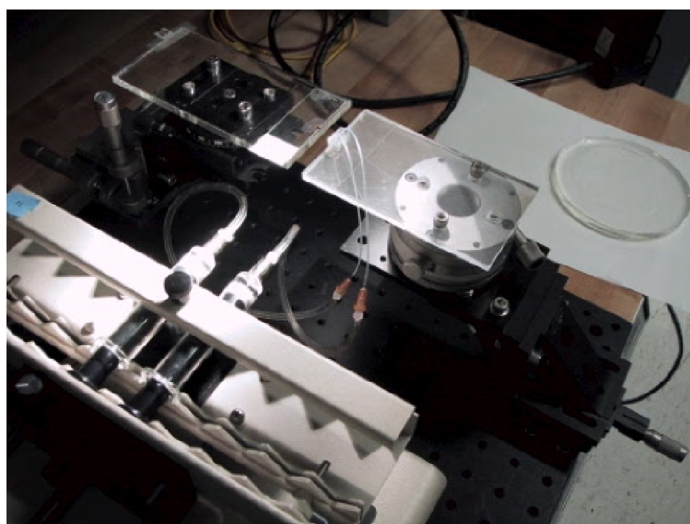

Figure 5.2.6. Syringe pump and alignment test setup

In order to test the practical use of our devices, we have tried to insert previously fabricated cantilevers from another research project into our channel device. A small shoulder on the PDMS protruding over the edge of the glass slide (Figure 5.2.7.) has been very useful for vertical alignment "by eye". We also observed that an increase in channel height will make the alignment process easier and therefore we decided to make higher channels next time.

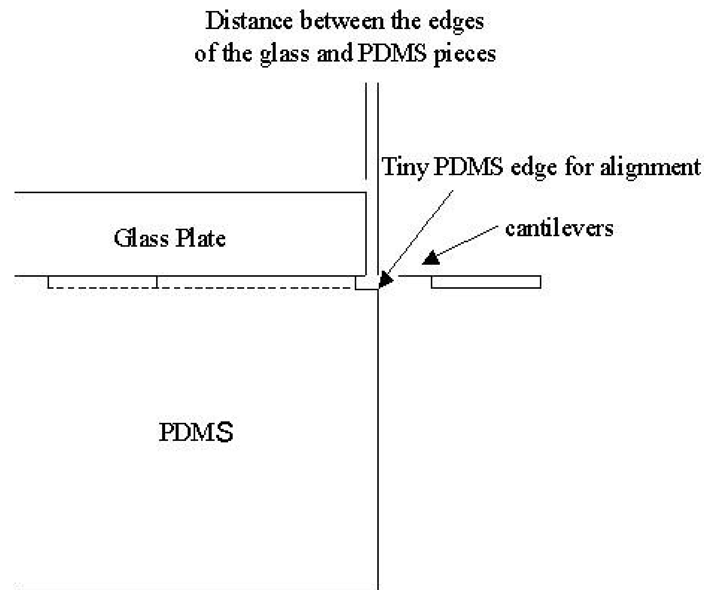

Figure 5.2.7. Cantilever alignment

After investigating the topography of the master wafers with an optical profilometer, we found the thickness of SU-8 layer to be about 40-44mm. We have also tried to measure the channel depth directly on the PDMS, but due to its transparency it was not possible to get viable data with this metrology device.

To increase the thickness of the SU-8 layer, one strategy is to double coat: after the first spin coating using the recipe mentioned earlier, the wafer was postbaked for about 20min at a temperature somewhat lower than 60 C, then it was coated again with SU-8 using the same spinning procedure, and baked according to the recipe. Another strategy is to reduce the spinning speed: we tried to decrease the spinning speed from 3000 rpm to 1000 rpm. We didn't really experiment with several different spin speeds, but such an experiment can be done to achieve a full table or plot of the thickness vs. spin speed, which would be a very good reference for future use. Both of these strategies have been proven to work since we measured SU-8 layers to be about 80-88mm on from both methods. Considering the possibility of putting even more that two layers of SU-8 onto a wafer, we could increase the channel height to virtually any value.

5.3 Recommendations and Conclusions

1. Thickness of the PDMS layer:

In our case, a thicker PDMS layer makes it easier to secure the tubing, but it also makes it hard to punch straight and smooth holes. Furthermore, a thicker PDMS is difficult to dice straight using razorblades. The thickness of our device that we felt comfortable with is about 8mm. An appropriate needle size has to be chosen for punching the holes. We would have liked to have experimented with making channels of variable depth, perhaps deeper at the spout. This would have been accomplished using at least two transparency masks, aligned to each other. The first mask would be the same as before, but the subsequent maskings would only expose the spout area, thus building up layers of SU-8 at the spout. The PDMS master would copy the topography, producing a deeper region near the spout than elsewhere in the channel.

2. Air plasma treatment:

The status of the plasma (air pressure, RF power…) and timing is important for proper strength of the adhesion between the PDMS and glass pieces. Depending on different ashers used, a lot of experience is needed to predict and improve the results. It was generally found that using higher power setting for about a minute properly prepared the surface; aiming for a magenta colored plasma.

3. Bonding procedure:

Since the adhesion strength is directly proportional to the cleanliness of the binding surfaces, the bonding procedure should be given due planning.

Full release of the devices began with a rough cut to remove a few devices, to comfortably fit on a single glass slide. This rough cut may be done with a razor blade or preferably a sharp scalpel, with the incision made from the channel-side of the mold. This rough cut should aim to bisect the cavity furthest from the spouts.

We prepared the PDMS and slide as described in the fabrication section. The ashed PDMS mold was lain face up, bringing the glass slide into contact from above, positioning it such that as much of the cavity overhung the edge of the slide, with as much of the spouts on the slide. We pressed the pieces until they bonded securely. Using the glass edge as a guide and cutting from the channel-side, cut the PDMS mold as cleanly as possible with a sharp scalpel in a single, smooth incision. This should achieve as fully-exposed spout area as possible for insertion, without allowing any fluid to pool on the glass surface.

4. Punching the holes:

To punch the holes straightly, a transparent plastic piece (~ 10mm thick) could with holes bored to ensure that the needle is square to the top surface, as shown in Figure 5.3.1. Due to time constraints, however, it was not possible for us to

prepare such a template device.

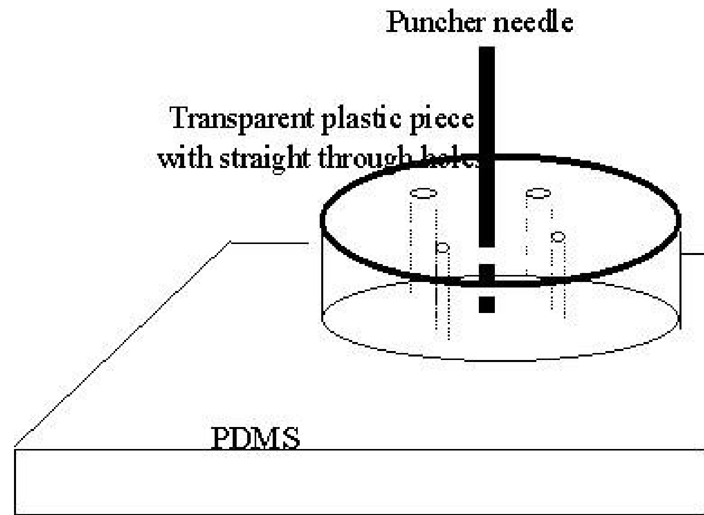

5. Dicing:

Give careful thought to the arrangement of the device units on the transparency. Position the devices on the transparency in such a way that many of them can be released in as few cuts as possible. We positioned our devices as shown in figure (5.3.2), so as minimize the amount of cutting to release several identical devices. Our design involved two reservoirs, each with its own spout. However, a large cavity was patterned above the spouts to simplify alignment to the edge of the glass slide. This strategy would be most useful in mass-production, but in research it would be best to position the devices as shown in figure (5.3.3), because it releases as all device types in 4 cuts as compared to 6 cuts as in figure (5.3.2). The most important cut is the spouts-release cut perpendicular to the spouts, just above the spouts. This cut should perform from the device side using a sharp blade against a straight edge against relaxed PDMS. Since the exposure field is a circle of 80mm diameter, many different types of devices can be arranged to be produced through a single exposure. Placing an asymmetric marking on the transparency will help in determining which side has ink on it when performing SU-8 photolithography.

An appropriate tool cut be made to cut the individual dies of the PDMS. In our case, a sharp and precise cut especially near the fluid spouts is needed for proper function. A sharp hollow puncher (like a cookie cutter, as shown in Figure 5.3.4.) with the size and shape of the frame of a single die of mirco channels might be more repeatable and faster than a simple razor blade.

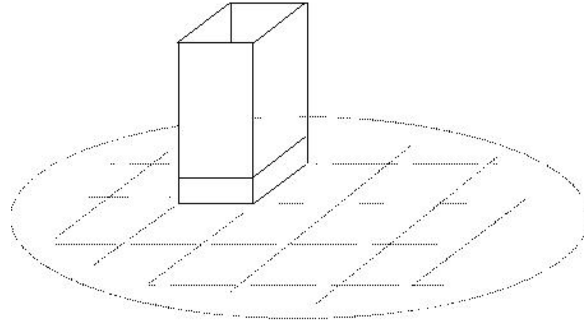

Figure 5.3.4.: "Cookie cutter"

6. Tubing attachment:

It is important to choose the proper combination of needle and the tubing diameters. The needle should be somewhat smaller than the tubing in order to achieve a tightly sealing fit. The tubing also needs to be made of sufficiently stiff material in order to facilitate the insertion process. This tubing must, in turn, be snuggly connected to the syringe.

7. Fabrication Planning:

The entire process, starting with the transparency masks, can be performed in a single day. Plan ahead to ensure all chemicals have been located and that proper machine reservations have been made. Begin early with the development of the SU-8, and plan the PDMS formation to occur in the afternoon. It was found that the silanizing agent was the most precious ingredient. Though very little of the agent is required to properly bond the SU-8 to the silicon substrate, the 2 hour vacuum desiccation step should be planned to occur during lunchtime.

8. Design Suggestions:

SU-8 is a negative photoresist. The pattern that is used to form the SU-8 should be transparent where one wants there to be a cavity. Figure (5.3.5). Our first attempt resulted in producing an inverted SU-8 pattern.

Figure (5.3.5)

Transparency Mask

□ **Channel cavity**

■ **PDMS formation**

The reservoirs should be designed to be very large. Ours were designed as 3mm diameter circles. Puncturing the PDMS mold for fluidic tubing would have been easier if the reservoirs were at least twice as big.

We have produced a working prototype of the microfluidic channel and formulated a process plan for fabricating many more.

PDMS Microchannel Fabrication Process Flow

General Purpose: To create simple microfluidic devices in PDMS with feature sizes greater than or equal to ~25 microns.

Notes: This process flow is to be executed in the EML. Pageworks transparencies are not to be taken into the ICL or TRL, but chrome masks can be made from transparencies that can be used in the ICL or TRL (see the additional resources at the end). This process flow is for rapid-prototyping, going from conception to final product in less than a week.

1 Fabrication of Transparency Mask

The vendor who we have typically used for outputting electronic files to emulsion transparencies (via. a laser-assisted imagesetter) is:

Pageworks 501 Cambridge Street Cambridge, MA 02141
Phone: (617) 374 - 6000
Fax: (617) 374 - 6020
http://www.pageworks.com

You will need to set up an account with Pageworks. Download the Prepress Output form from the web.

Pageworks can work with many types of files (check their webpage or call for details); however, we have had most success with using the graphics application, Macromedia Freehand 9.0 (~$85, academic version). Please note that this is not a technical drawing program but it can be used successfully with larger geometries. You need only save your file as a standard Freehand 9.0 file (*.fh9). It is best to change the default units in Freehand to millimeters for working with micrometer dimensions. Select all the objects on your mask and group them together.

Save file. Print your file on a laser printer and examine for nominal adherence to your expectations. Save the file as *.fh9 and follow the directions below.

Once you've prepared your file, you're ready to send it out to be printed (most of these details are available on the Pageworks webpage).

1.1 Submit your file to Pageworks. Log onto their anonymous ftp website at ftp://ftp.pageworks.com/. Login as anonymous and use your email address for the password. Drop your file off in the incoming folder.

1.2 Then, either download the Prepress Order Form from their website, complete it and fax it back to them, or fill out their online Prepress Order Form. Each page is $19.95 + $6.10 (if you have delivered by the Pageworks Courier). Most of the order form is self-explanatory, the only questions that may arise are around the section, Output Type, and the options are:

1.2.1 Media: RC Paper/film pos/film neg
You want either "film pos" or "film neg" depending if you want a clear field or dark field mask. "film pos" produces a transparency that looks like the image on the monitor & "film neg" produces a transparency that is the inverse of the image on the monitor. If you are using SU-8 as the master, you will want "film neg" because this is a negative PR.
1.2.2 Emulsion: down/up
This tells them whether you want the emulsion on the front or backside of the transparency -- you will bring the emulsion side into contact with the resist-coated wafer (to ensure good pattern transfer). So think now about which orientation you need.
1.2.3 Resolution: 1270/2540/3386/5080
5080 is what you want -- highest resolution (consult with Pageworks).
1.2.4 Leave the rest of the boxes blank: they deal with color images. If you have questions, talk with the Pageworks folks.

1.3 If you submit your job by 6 p.m. (weekdays), the job will be ready and delivered to your door (if you requested that) by 9 - 10 a.m. the following morning. Call Pageworks to confirm that they have received your file. You're now ready to transfer your transparency to the wafer.

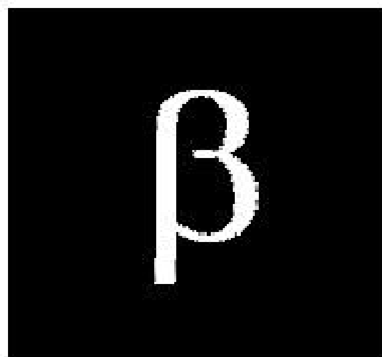

2 Fabrication of Silicon Master

STANDARD OPERATING PROCEDURE (adapted)
SU-8 (50): Negative, Epoxy-based Resist developed by IBM (EML)

INTRODUCTION:

This procedure describes the use of SU - 8 (a negative, epoxy-based resist developed by IBM). The MSDS sheets for this material can be found in the copier room on the second floor of Building 39.There are many variations on the procedure described here that are practiced for making SU- 8 microstructures - these are parameters that have worked for us. Coating and developing of SU-8 is carried out in the pispinner hood.

SAFETY:

Follow the standard safety procedures associated with the use of the pispinner and solvents.

PROCEDURE:

2.1 Log into the EML computer station upon entering the lab. Check equipment reservations to ensure that you reserved the correct machine(s) in the correct facilities for the correct date. Another user may have reservations and it is your responsibility to honor them, if this is the case.

2.2 To ensure good adhesion of the SU-8 to your wafer, you need to do a dehydration bake. Use the hotplates (currently located in the PR room under the hood). We use the plate with the metal top for the dehydration step to promote planar thermal contact. Place the wafers on the hot plate and set the temperature to 200 degrees Celsius. SOP for the newer hotplate: with RT shown, press ENT key, press “plate temp”, press desired temperature (eg. 2-0-0), then press ENT. They should be dehydrated for at least 20 minutes immediately prior to coating SU-8. Note: these wafers are “green dot” - if you're working with gold-contaminated wafers then you need to use a spacer wafer to minimize contamination of the plates.

2.3 In the meantime, prepare the pispinner (see SOP for pispinner if you're unclear on its use). Remember to coat the spinner bowl with aluminum foil or with fabwipes (be sure to secure them). Choose the appropriate chuck (depends on the level of contamination of the wafers and the size of the piece). Using a dummy wafer, set the spin-speeds and times. To coat a film of SU-8 approximately 60 microns, start at 500rpm for 10s and increase to 3000rpm for a total of 30s. To coat a film of SU-8 approximately 80

microns, start at 500rpm for 10s and increase to 1500rpm for a total of 30s. Make sure that the acceleration adjustment is turned to it's maximum. After spinning is complete, use a Q-tip to remove the resist attached to the rim of the wafer.

2.4 Blow off wafers with nitrogen then place your wafer on the chuck and confirm that it's centered and that the spin-speeds and times are correctly set. Pour SU-8 from the bottle so that a drop about 2" diameter is on the wafer. Try not to introduce bubbles as you pour the resist - please clean up the bottle after pouring (with a fabwipe). Start the spinning cycle.

2.5 Use the wafer tweezers to move the wafer to one of the metal-topped hotplates (don't use the ceramic hotplate because it is not very flat on top). The edge of the wafer isn't exposed anyway, so the marks in the resist are tolerated. Turn the hotplate on and ramp the temperature up to 105 degrees Celsius (from room temperature it will take about 7-8 minutes). Hold the temperature at 105 degrees Celsius for 15 minutes and then allow cooling. Leave the wafer on the hotplate until it is down to at least 60 degrees Celsius (i.e., below the glass transition temperature of SU-8).

2.6 The wafer is now ready to be exposed. Using the ksaligner in the EML, you can expose the resist as follows. Place a glass slide in the mask chuck. Place the wafer in the wafer chuck (SU-8 towards exposure) and lay the transparency mask (ink towards SU-8) on the wafer. Carefully slide the wafer-mask assembly into the exposure field, trying to avoid moving the mask in bring mask into contact by rotating the lever away from the user. We have had success with exposure times of about 2 minutes on the EML aligner.

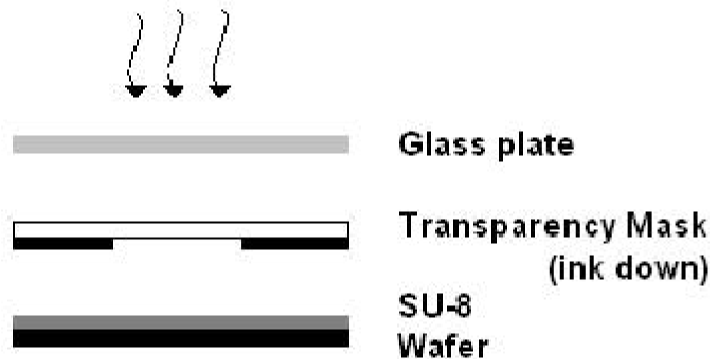

2.7 After exposure, you need to do a post-exposure bake on the metal-topped hotplate to cross-link the exposed resist. We typically use the same heating schedule as for the initial bake. Heat up to 105 C from room temperature, hold at 105 C for 15 minutes, and then allow to cool down to at least 60C.

2.8 To develop the resist, select a Pyrex container that is appropriate for the contamination level of the wafer. Under hood, pour SU-8 developer (PGMEA) (it can be found in the solvent pass-through) into the container. Place wafer into the developer and agitate as for regular resist. The resist will take about 5 minutes to develop. Once the resist has developed, rinse the wafers with fresh PGMEA (SU-8 developer) and blow them dry with nitrogen.

2.9 If you have only used the developer for a couple of wafers, then place it into the container in the pass-through marked "SU-8 Developer- Used but not Waste". Otherwise, place it into the dedicated SU-8 waste bottle. Rinse the developing beaker with PGMEA (3 times), then IPA and place it next to the sink to dry.

2.10 Clean up the pispinner and hood. Please leave it in the state you found it. The SU-8 coated wafer is now stable and can be stored.

3 Fabrication of PDMS Fluidic Channels & Assembly of Devices

3.1 The silanizing agent should be placed in a small metal sample holder and the wafer coated with SU-8 placed on top of the holder, covering the silanizing agent. The holder-wafer assembly should be placed in a vacuum dessicator for 2 hours.

3.2 Mix the PDMS (also called Sylgard 184) prepolymer components (10:1) and degas under vacuum for 20 minutes.

3.3 Place the wafer in a glass or tough plastic petri dish and carefully pour the PDMS over it. Try not to introduce too many bubbles while pouring.

3.4 Cure the PDMS in the pre-treat oven at the back of the EML photolithography room for at least an hour. The oven should be set to 90 degrees. After curing, the PDMS should be hard to the touch. The wafer with SU-8 and PDMS is again stable and may be stored.

3.5 Clean up the various workstations and log out of the EML computer system. The remaining processing steps were executed in the Nanoscale laboratory in the Media Lab.

3.6 Peel off the PDMS mold from the silicon master, and cut it to the desired shape. Use a medical coring syringe to punch holes for fluidic interconnects. This is best done on a cardboard surface so the coring syringe punctures the PDMS and also pierces the cardboard - this ensures a clean cut of the PDMS with minimal flash.

3.7 Clean the PDMS mold with Scotch Tape.

3.8 Place a clean glass slide and the PDMS mold in an air plasma asher with the surfaces to be bonded exposed to the plasma. This step may require trial and error to determine the ideal power/time settings. The plasma should be magenta colored. It has been found that 60s on HIGH setting works well using the plasma asher in the Nanoscale Lab.

3.9 Carefully attach the PDMS mold to the glass slide, laying it down to avoid capturing air bubbles (it should adhere strongly so you will only get one chance at this).

3.10 Insert tubing into holes. The tubing should be chosen such that it fits snuggly into the holes punched by the coring syringes.

3.11 The microfluidic channel fabrication is now complete. Clean up your workstation.

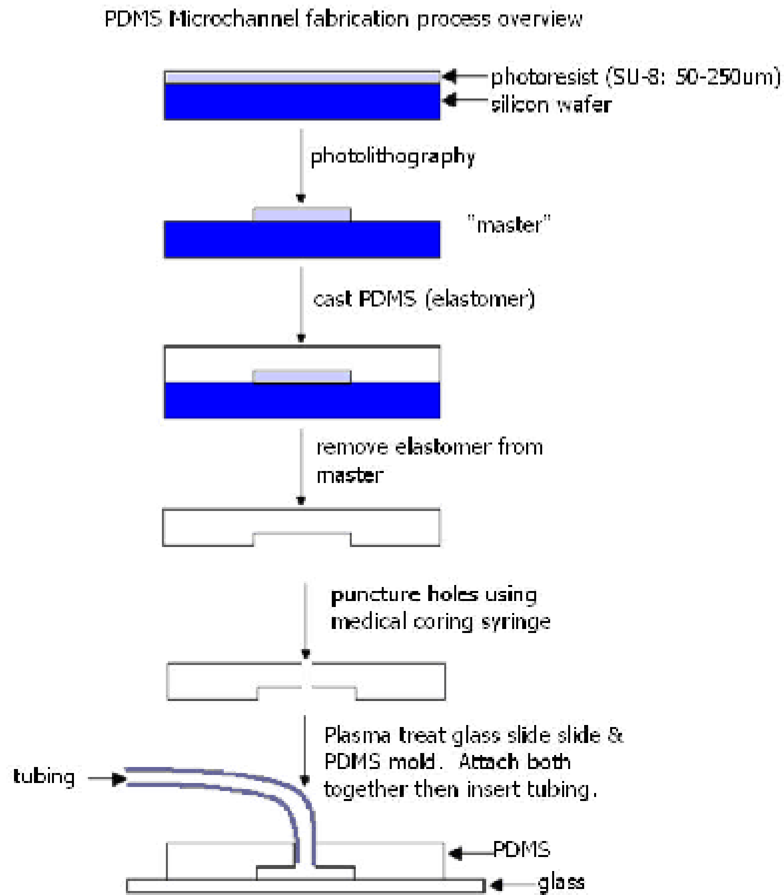

Written by Dean Berlin (dberlin@mit.edu).

Other contacts:

Wan-Chen Wu (wcwu@mit.edu)
Bill Teynor (solarboy@mtl.mit.edu)
Dr. Rebecca Jackman (rjackman@mit.edu)
Sameer Ajmera (ajmers@mit.edu)

Additional Resources:

SOP for SU-8
SOP for PDMS
SOP for Preparation of Chrome Masks from Emulsion Transparencies (TRL)
Course webpage for IAP 2001 BioMEMS Short Course taught by Prof. Martin Schmidt, Dr. Rebecca Jackman, and Hang Lu.

5/14/2001

REFERENCES

[1] J. Fritz, M.K. Baller, H.P. Lang, T. Strunz, E. Meyer, H.-J. Guntherodt, E. Delamarche, Ch. Gerber, J.K. Gimzewski, "Stress at the Solid-Liquid Interface of Self-Assembled Monolayers on Gold Investigated with a Nanomechanical Sensor," American Chemical Society (2000).

[2] J. Fritz, M.K. Baller, H.P. Lang, H. Rothuizen, P. Vettiger, E. Meyer, H.-J. Guntherodt, Ch. Gerber, J.K. Gimzewski, "Translating Biomolecular Recognition into Nanomechanics," Science 288 316 (2000).

[3] J. Thaysen, R. Marie, A. Boisen, "Cantilever Based Bio-Mechanical Sensor Integrated in a Microliquid Handling System", Conference Proceedings MEMS 2001, p.410-404, January 2001

[4] E.B. Cooper, E.R. Post, S. Griffith, J. Levitan, S.R. Manalis, M.A. Schmidt, C.F. Quate, "High-resolution micromachined interferometric accelerometer,"Applied Physics Letters, 76 3316 (2000).

[5] David C. Duffy, J. Cooper McDonald, Olivier J.A. Schueller, and George M. Whitesides, "Rapid Prototyping of Microfluidic Systems in Poly(dimethylsiloxane)," Anal. Chem. 70, 4974-4984 (1998).

[6] Rebecca Jackman, "Fabrication of PDMS-Based BioMEMS," Presentation given in MIT IAP 2000 BioMems class (2000).

[7] M.K. Baller, H.P. Lang, J. Fritz, Ch. Gerber, J.K. Gimzewski, U. Drechsler, H. Rothuizen, M. Despont, P. Vettiger, F.M. Battiston, J.P. Ramseyer, P. Fornaro, E. Meyer, H.-J. Guntherodt,"A Cantilever Array-Based Artificial Nose," Ultramicroscopy 82 (2000).

[8] R. Berger, E. Delamarche, H.P. Long, C. Gerber, J.K. Gimzewski, E. Meyer, H.J. Guntherodt, "Surface Stress in the Self-Assembly of Alkanethiols on Gold," Science 276 2021 (1997).

[9] A.M. Moulin, S.J. O'Shea, R.A. Bradley, P. Doyle, M.E. Welland, "Measuring Surface Induced Conformational Changes in Proteins," Langmuir 15 8116 (1999).

[10] R. Raiteri, H.-J. Butt, M. Grattarola, "Changes in surface stress at the liquid/solid interface measured with a microcantilever," Electromechanica Acta 46 157 (2000).

[11] J. Fritz, M.K. Baller, H.P. Lang, H. Rothuizen, P. Vettiger, E. Meyer, H.-J. Guntherodt, Ch. Gerber, J.K. Gimzewski, "Translating Biomolecular Recognition into Nanomechanics," Science 288 316 (2000).

[12] J. Fritz, M.K. Baller, H.P. Lang, T. Strunz, E. Meyer, H.-J. Guntherodt, E. Delamarche, Ch. Gerber, J.K. Gimzewski, "Stress at the Solid-Liquid Interface of Self-Assembled Monolayers on Gold Investigated with a Nanomechanical Sensor," American Chemical Society (2000).

[13] H.F. Ji, K.M. Hansen, Z. Hu, T. Thundat, "Detection of pH Variation Using Modified Microcantilever Sensors," Sensors and Actuators B72 233 (2001).

[14] T. Thundat, E. Finot, Z. Hu, R.H. Ritchie, G. Wu, A. Majumdar, "Chemical Sensing in Fourier Space," Applied Physics Letters 77 4061 (2000).

[15] S.R. Manalis, S.C. Minne, A. Atalar, C.F. Quate, "Interdigital Cantilevers for Atomic Force Microscopy," Applied Physics Letters, 69 3944 (1996).

[16] G.G. Yaralioglu, A. Atalar, S.R. Manalis, C.F. Quate, "Analysis and Design of an Interdigital Cantilever as a Displacement Sensor," Journal of Applied Physics 83 7405 (1998).

[17] M.Mao, T. Perazzo, O. Kwon, A. Majumdar, J. Varesi, P. Norton, "Direct-View Uncooled Micro-Optomechanical Infrared Camera" IEEE 100 (1999).

[18] Fu, A. Y. et al. 1999. A Microfabricated Fluorescence-Activated Cell Sorter. *Nature Biotechnology.* 17:1109-1111.

[19] Jackman, R. J. et al. 1998. Fabricating Large Arrays of Microwells with Arbitrary Dimensions and Filling Them Using Discontinuous Dewetting. *Anal. Chem.* 70: 2280-2287.

[20] Kenis, P. J., Ismagilov, R. F., and Whitesides, G. M. 1999. Microfabrication inside Capillaries Using Multiphase Laminar Flow Patterning. *Science*. 285: 83-85.

[21] Voldman, J., Gray, M. L., and Schmidt, M. A. 1999. Microfabrication in Biology and Medicine. *Annu. Rev. Miomed. Eng.* 01: 401-425.

[22] Xia, Y. and Whitesides, G. M. 1998. Soft Lithography. *Annu. Rev. Mater. Sci.* 28:153-184.